



HAL
open science

Soil structure as an indicator of soil functions: A review

Eva Rabot, Martin Wiesmeier, Steffen Schlüter, Hans-Jörg Vogel

► To cite this version:

Eva Rabot, Martin Wiesmeier, Steffen Schlüter, Hans-Jörg Vogel. Soil structure as an indicator of soil functions: A review. *Geoderma*, 2018, 314, pp.122-137. 10.1016/j.geoderma.2017.11.009. hal-03858205

HAL Id: hal-03858205

<https://hal.science/hal-03858205>

Submitted on 5 Sep 2023

HAL is a multi-disciplinary open access archive for the deposit and dissemination of scientific research documents, whether they are published or not. The documents may come from teaching and research institutions in France or abroad, or from public or private research centers.

L'archive ouverte pluridisciplinaire **HAL**, est destinée au dépôt et à la diffusion de documents scientifiques de niveau recherche, publiés ou non, émanant des établissements d'enseignement et de recherche français ou étrangers, des laboratoires publics ou privés.



Distributed under a Creative Commons Attribution - NonCommercial - NoDerivatives 4.0 International License

Soil structure as an indicator of soil functions: A review

E. Rabot^a, M. Wiesmeier^b, S. Schlüter^a, H.-J. Vogel^{a,*}

^a Helmholtz Centre for Environmental Research – UFZ, Department of Soil System Science, Halle (Saale), Germany

^b Chair of Soil Science, TUM School of Life Sciences Weihenstephan, Technical University of Munich, Freising, Germany

* Corresponding author: hans-joerg.vogel@ufz.de (H.-J. Vogel)

Abstract

Since many processes in soil are highly sensitive to soil structure, this review intends to evaluate the potential of observable soil structural attributes to be used in the assessment of soil functions. We focus on the biomass production, storage and filtering of water, storage and recycling of nutrients, carbon storage, habitat for biological activity, and physical stability and support. A selection of frequently used soil structural properties are analyzed and discussed from a methodological point of view and with respect to their relevance to soil functions. These are properties extracted from soil profile description, visual soil assessment, aggregate size and stability analysis, bulk density, mercury porosimetry, water retention curve, gas adsorption, and imaging techniques. We highlight the greater relevance of the pore network characterization as compared to the aggregate perspective. We identify porosity, macroporosity, pore distances, and pore connectivity derived from imaging techniques as being the most relevant indicators for several soil functions. Since imaging techniques are not widely accessible, we suggest using this technique to build up an open access “soil structure library” for a large range of soil types, which could form the basis to relate more easily available measures to pore structural attributes in a site-specific way (i.e., taking into account texture, soil organic matter content, etc.).

Keywords: Visual soil assessment; Aggregate size distribution and stability; Bulk density; Mercury porosimetry; Water retention curve; Imaging techniques

Abbreviations: BD, bulk density; DC, degree of compactness; LLWR: least limiting water range; MIP: mercury intrusion porosimetry; SOM, soil organic matter

1. Introduction

Soil structure is recognized to control many processes in soils. It regulates water retention and infiltration, gaseous exchanges, soil organic matter and nutrient dynamics, root penetration, and susceptibility to erosion. Soil structure also constitutes the habitat for a myriad of soil

organisms, consequently driving their diversity and regulating their activity (Elliott and Coleman, 1988). As an important feedback, soil structure is actively shaped by these organisms, thus modifying the distribution of water and air in their habitats (Bottinelli et al., 2015; Feeney et al., 2006; Young et al., 2008). Since many processes in soil proved to be linked to soil structure, this review intends to evaluate the potential of soil structure to be used in the assessment of soil functions. We refer to soil structure as the spatial arrangement of solids and voids across different scales without considering the chemical heterogeneity of the solid phase. Thus, the solid phase and pore space are complementary aspects of soil structure which can be approached from both perspectives.

The solid phase perspective, based on mechanisms of soil aggregation, has been supported by Tisdall and Oades (1982). Since their pioneering work, aggregation is conceptually viewed as a three-stage hierarchical organization of the soil solid phase, each stage involving characteristic binding agents. Primary particles ($< 20 \mu\text{m}$) are bound together into microaggregates ($20\text{--}250 \mu\text{m}$), which are bound together to form macroaggregates ($> 250 \mu\text{m}$). Follow-up studies favored a different sequence of aggregate formation: macroaggregates can form around particulate organic matter, then microaggregates are released upon breakdown of macroaggregates (Angers et al., 1997; Oades, 1984). The bonds within microaggregates are supposed to be more persistent than those between macroaggregates (Tisdall and Oades, 1982). This hierarchical order, responsible for the micro- and macroaggregate formation, was identified in soils where soil organic matter was the major binding agent, but could neither be found in oxide-rich nor in sandy soils (Christensen, 2001; Oades and Waters, 1991; Six et al., 2004).

Following a pore perspective, soil structure may not be defined as “the shape, size and spatial arrangement of primary soil particles and aggregates” but as “the combination of different types of pores” (Pagliai and Vignozzi, 2002), where surfaces of soil particles are assumed to be the walls of the pore space (Elliott and Coleman, 1988). Similar to the aggregate hierarchy, a hierarchy of pores can be defined (Elliott and Coleman, 1988). Depending on their size, pores are classified as macropores, mesopores, and micropores, although there are no generally agreed upon size thresholds between these categories. Pores resulting from the arrangement of soil primary particles are called textural pores, whereas bigger pores resulting from biological activity, climate, and management practices are called structural pores.

These two different perspectives rely on the perception of what is actively shaped: aggregates or pores. Considering the multitude of soil processes and their interactions, there is ample

evidence that generally both are possible with changing balance depending on soil type and site conditions. Irrespective of these different perspectives, there are distinct methods available to characterize either the solid phase arrangement or the pore space, and the obtained results are expected to differ in sensitivity, cost, or relevance to soil functions.

Yet, there is no universally accepted way to characterize soil structure (Díaz-Zorita et al., 2002), and this is even more true for using soil structural measures as indicators for soil functions as we intend to do. Wallace (2007) describes ecosystem functions as a synonym of ecosystem processes. Therefore, soil functions refer to “what the soil does” (Seybold et al., 1998), i.e., intrinsic processes occurring in soils irrespective of any human interest. From this definition, we assume that it is possible to assess soil functions through information-bearing soil properties called indicators. Good indicators must be highly correlated with the function of interest (Reinhart et al., 2015), that is to say, with other soil properties governing soil processes (e.g., saturated hydraulic conductivity, air permeability, etc.). Their measurement must be reliable and reproducible. The monetary and human costs for their acquisition and the level of expertise needed are also important aspects. A wide number of methods and structural properties are currently used by soil scientists and farmers, from quick field observations to thorough laboratory characterizations. Our intention is to provide a critical analysis of their efficiencies as related to soil functions.

We will particularly focus on six soil functions: biomass production, storage and filtering of water, storage and recycling of nutrients, carbon storage, habitat for biological activity, and physical stability and support. Attention will be paid on structural soil properties representative at the scale of pedons and soil horizons, assuming that soil functions can be assessed for 1-D soil profiles in a meaningful way. Since it is essential that the methods used be reliable from a technical point of view, we will discuss corresponding advantages and limitations. We will also report to what extent simple methods can substitute more complex ones to find a trade-off between reliability of information and acquisition cost. We will evaluate the different methods in terms of sampling requirements, reproducibility, cost, and level of expertise required. We chose to separate the available approaches to characterize soil structure based on the solid phase arrangement from those based on the pore space perspective.

2. Characterization of the solid phase arrangement

2.1. Field methods

Methods available to characterize soil structure directly in the field mainly aim at describing the “macrostructure”, that is to say, visible to the naked eye (Baize et al., 2013). They can roughly be divided in two groups: the whole profile evaluation, developed from the fundamental methods of field surveys, and the topsoil evaluation, a simplified version especially designed for farmers.

2.1.1. Whole profile evaluations

Following the FAO (2006) guidelines and most of the national standards (e.g., Ad-hoc-AG Boden, 2005 in Germany; Baize and Jabiol, 2011 in France; Schoeneberger et al., 2012 in the USA), soil structure morphology and its variation with depth are evaluated visually as part of the soil profile description. The description of soil structure is mainly related to its grade, and the size and shape of aggregates (Ad-hoc-AG Boden, 2005; Baize and Jabiol, 2011; FAO, 2006; Schoeneberger et al., 2012). The term aggregates usually comprises peds, fragments, and clods. Aggregates formed by natural processes are called peds, small aggregates formed artificially during laboratory or field manipulations are called fragments, and large aggregates formed artificially by cultivation operations are called clods. When soil material breaks into aggregates of higher order than the single grains (pedal soils), structure can be addressed by describing the grade of these aggregates. The grade describes the distinctness of the aggregates in place, qualified as strong, moderate, or weak. Qualifying the grade is realized by observing whether soil material breaks into fragments or “powder” when disturbed, and to what extent the surface of aggregates differs from their inner part (FAO, 2006). The aggregate shape is described according to several types of soil structure: among others, angular blocky, subangular blocky, granular, platy, prismatic, or columnar. In structureless soils (apedal soils), no aggregate are observed and the material is either compact or built up by single grains. Another approach is to distinguish soil clods based on a visual inspection of their internal structural porosity (Boizard et al., 2017; Roger-Estrade et al., 2004). It has to be noted that the size, abundance, orientation, and continuity of voids can be described in the field, with the naked eye or a hand-lens. However, the description of the complete void organization cannot be done (Baize and Jabiol, 2011).

The description of soil structure in the field highly depends on soil moisture, especially in swell-shrinking soils. Therefore, the FAO (2006) guidelines recommend performing this description

when the soil is dry or slightly moist. The whole profile evaluations provide valuable information on the vertical sequence of soil structural properties. However, they are subjective, and since they require the digging of pits, they are also time consuming, and sufficient replication cannot always be done (Mueller et al., 2009).

Field observations of aggregate size, shape, and grade are rarely used as indicators for soil functions. Pulido Moncada et al. (2014c) used the aggregate shape (FAO, 2006) and showed that it was sensitive to soil type for the two studied soils, but poorly sensitive to land use (in this study, cereal monoculture vs. permanent pasture). By applying regression trees on a database gathering water retention measurements and field descriptions of soil structure, Pachepsky and Rawls (2003) found that the grade of soil structure, classified as strong, moderate, or weak, was the most informative to explain the water retention values, followed by the aggregates size and shape. In this case, water retention was correlated with the grade, because of the water capacity of small intra-aggregate pores. However, the overall discriminating power of the aggregate grade, size, and shape depended on the texture class.

2.1.2. Topsoil evaluation

Because accurate soil profile description requires considerable experience, simplified approaches based on field tests were designed to assess physical properties visually (Shepherd, 2000). They are particularly developed to estimate soil quality and are highly relevant for farmers or land managers, who wish to evaluate the quality of their soils and their management practices, easily, quickly, and cheaply. Indeed, the evaluation is often performed in < 20 min, with a spade being the main required equipment. Several “spade tests” were proposed, such as the Peerlkamp (1959) test, the “Visual Evaluation of Soil Structure” (Ball et al., 2007; Guimarães et al., 2011), the “Visual Soil Assessment” (Shepherd, 2009, 2000), or the “SOILpak score” (McKenzie, 2001). A similar approach exists for subsoil (Ball et al., 2015). In the topsoil evaluations, an undisturbed soil block is extracted from soil surface with a spade (e.g., full size of the spade and approximately 20 cm-thick) and manually broken or dropped from a 1 m-height to produce aggregates. Aggregates are then described in terms of size, porosity, shape, color, ease of breakup, together with the identification of the presence of a tillage pan, depth of root penetration, or number of earthworms. The soil samples are then compared to the photographs of a reference key to score soil structure (Figure 1).

These visual soil evaluation methods usually demonstrated a good sensitivity to different management practices (Ball et al., 2007; Giarola et al., 2013; Guimarães et al., 2011), and were

particularly useful to detect soil compaction. Scores were correlated to the agricultural productivity function (Mueller et al., 2009), to water infiltration through the saturated hydraulic conductivity (Mueller et al., 2009; Pulido Moncada et al., 2014b; Shepherd, 2003), and to gas transport through the air permeability and air capacity (Guimarães et al., 2013; Shepherd, 2003). A “good” soil structure, according to the visual soil evaluation scores, was associated with a low soil BD, low penetration resistance, low tensile strength, low compaction state as estimated with the degree of compactness, or high number of pore branches (Garbout et al., 2013; Guimarães et al., 2013, 2011; Mueller et al., 2009; Newell-Price et al., 2013; Pulido Moncada et al., 2014b). However, when compared, the different visual soil evaluation methods sometimes led to very different results in terms of soil physical quality (Giarola et al., 2013; Mueller et al., 2009; Newell-Price et al., 2013).

Methods of visual soil evaluation remain poorly used in research, because they are operator dependent and only provide semi-quantitative results. The main drawback is the considerable subjectivity introduced, for example, by the scoring with a reference to photographs. In addition, when the method requires to break the soil manually to produce aggregates (e.g., Ball et al., 2007), the results depend on the experience of the operator (Giarola et al., 2013; Guimarães et al., 2011). In order to standardize this procedure, Shepherd (2009, 2000) rather uses the drop-shatter test, where the soil block is dropped from a 1 m-height on a wooden board, a maximum of three times. However, mixing the soil by using the drop-shatter test or calculating the weighted mean of each layer score (e.g., Ball et al., 2007) reduces the efficiency of the visual soil evaluation when contrasting layers, potentially limiting for some soil functions, are present (Newell-Price et al., 2013; Pulido Moncada et al., 2014c). It has been recognized that the results of such visual evaluations are sensitive to soil texture (Giarola et al., 2013; Newell-Price et al., 2013) since coarser, less cohesive soils, break up into finer fragments and get higher scores. Moreover, results depend on the actual soil water content (Guimarães et al., 2011) and on biological activity and consequently on the growing season (Mueller et al., 2009). Yet, the range of water content at which the evaluation is performed is not standardized (Guimarães et al., 2017).

2.2. Laboratory methods

In this section, we review structural soil properties obtained for soil samples collected in the field, then analyzed with more or less labor-intensive methods in the laboratory to characterize the solid phase arrangement.

2.2.1. Bulk density and derived indicators

One of the most prominent indicators of soil structure is soil bulk density (or dry bulk density), because it does not require any specific expertise or expensive equipment. It is calculated as the ratio of the dry mass of solids to the undisturbed soil volume. Porosity can then be derived from BD, knowing or approximating the particle density value. Samples of known volume are typically obtained by using cores (or volumetric rings) of well-defined size. Alternatives are the excavation and the clod methods which are more labor-intensive, since the sampled volume needs to be determined after extraction. In the excavation method, the volume is estimated by measuring the elevation of the ground surface before and after excavation (Soil Survey Staff, 2014), or by filling the hole left with water, sand, or another material (Frisbie et al., 2014; Laundré, 1989). The excavation method is particularly adapted for loose soils, where a coherent sample cannot be collected (Harrison et al., 2003). In the clod method, the clod is first coated or saturated with a water repellent substance (e.g., paraffin), and the volume is then determined by water displacement. This method can also be used to measure aggregate density (e.g., Rücknagel et al., 2007). Other variants of volume determination exist, such as photogrammetry (Bauer et al., 2014; Rossi et al., 2008) or the use of a pycnometer (Uteau et al., 2013). It is worth noting that some sensors were developed to estimate BD directly in the field to collect high amounts of data in a shorter period of time (Holmes et al., 2011; Lu et al., 2016; Timm et al., 2005). The soil water content and sometimes the particle size distribution need to be known to relate the sensor response to BD.

The various methods are prone to some errors in BD determination (Page-Dumroese et al., 1999). By definition, the clod method gives an inadequate representation of large pores, since inter-clod pores are not sampled. With the core method, soil compaction may occur during sampling (Håkansson, 1990; Page-Dumroese et al., 1999; Schlüter et al., 2011). Moreover, with small-diameter cores, the representative elementary volume with respect to soil structure may not be sampled (Page-Dumroese et al., 1999; Timm et al., 2005). Obtaining reliable BD measurements in soils with abundant rock fragments is recognized to be even more challenging. Indeed, the representative elementary volumes are very large (Vincent and Chadwick, 1994). Rocks can obstruct ring penetration and rock fragments larger than the cylinder diameter are excluded (Harrison et al., 2003; Page-Dumroese et al., 1999; Throop et al., 2012; Vincent and Chadwick, 1994). The excavation method is probably more efficient in this case (Harrison et al., 2003; Page-Dumroese et al., 1999). For swell-shrinking soils, the volume depends on the

water content during sampling, which should be well defined to get comparable results (Keller and Håkansson, 2010; Mueller et al., 2009).

BD is mainly considered to be useful to estimate soil compaction. Root length density, root diameter, and root mass were observed to decrease after an increase in BD (Dal Ferro et al., 2014). However, the interpretation of BD with respect to soil functions depends on soil type, especially soil texture and soil organic matter (SOM) content. Moreover, no strong link with the crop production function has been found, because the optimal BD for crop growth depends on soil texture and plant physiology (Kaufmann et al., 2010).

Some authors suggested using the degree of compactness (DC, also called relative BD) as a less site-specific, and therefore more powerful indicator of the compaction state of ploughed layers (e.g., da Silva et al., 1997; Håkansson, 1990; Håkansson and Lipiec, 2000). To remove the effect of soil type, DC is defined as the ratio of soil BD to the reference BD_{ref} of the same soil, which is thought to represent the maximum compaction that the soil can experience in field conditions. Yet, there is no standard procedure so that different values for BD_{ref} and DC are obtained (Håkansson, 1990; Naderi-Boldaji and Keller, 2016; Reichert et al., 2009). The normalization aims at removing the dependency of BD to clay and SOM content. It proved to be efficient under soils derived from similar parent materials and climatic conditions (da Silva et al., 1997). However, it was not satisfying for organic soils (Håkansson, 1990). A negative linear relationship was found between DC and macroporosity, and between DC and the logarithm of saturated hydraulic conductivity (Reichert et al., 2009). With respect to plant growth, an optimum function was defined by Reichert et al. (2009), who found the highest yields for DC values between 80 and 90%, but with considerable uncertainty due to the considered crop and the method used to define BD_{ref} (Reichert et al., 2009).

The packing density is another indicator derived from BD describing the state of compaction (Renger, 1970). A correction term is added to BD to account for the clay content in estimating the critical compaction with respect to crop growth. The correction term is defined as the product of the clay content and the slope of the regression between BD and clay content (Renger, 1970). A correction for the silt dependency can also be applied (Renger et al., 2008). In this way, it becomes possible to define a unique threshold of packing density to characterize optimal crop growth, valid for a variety of soil types. A packing density $< 1.7 \text{ g cm}^{-3}$ would be optimal for crop growth and limiting for crop growth when $> 1.7 \text{ g cm}^{-3}$ (Kaufmann et al., 2010). This parameter has been poorly explored so far.

2.2.2. Aggregate size distribution and stability

Another common way to characterize the solid phase arrangement and its supposed hierarchical orders is through the analysis of the aggregate-size distribution and aggregate stability, i.e., the ability of soil to retain its structure under the actions of water and mechanical stress (Dexter, 1988). In the laboratory, the aggregate size can be characterized more thoroughly than in the field (Section 2.1.1). Aggregates are broken to a number of size fractions following various protocols (Díaz-Zorita et al., 2002). During “dry sieving”, air- or oven-dried soil samples are sieved for a given duration or until complete separation. For “wet sieving”, dried, field moist, or rewetted soil samples are immersed in water or other solvents, and in some cases submitted to oscillations, and sieved. Some other protocols use a rainfall simulator (e.g., Almajmaie et al., 2017; Moebius et al., 2007). During wet sieving, aggregates are subjected to slaking due to fast wetting of dry aggregates, micro-cracking through differential swelling, or mechanical breakdown (Le Bissonnais, 1996). The proportion of fragments $> 250 \mu\text{m}$ constitutes the water-stable aggregates, whereas the $50\text{--}250 \mu\text{m}$ fraction represents the water-stable microaggregates (Dexter, 1988). Microaggregate stability is also studied by measuring the water-dispersible clay fraction (Brubaker et al., 1992; Calero et al., 2008; Czyż and Dexter, 2015; Paradelo et al., 2013).

Then, indices are computed to express the results (Díaz-Zorita et al., 2002). Aggregate size distribution is characterized after fitting a distribution function to obtain, for example, the mean weight diameter, the mean and standard deviation for a Gaussian, or the geometric mean diameter for a log-normal distribution. Aggregate stability is characterized by analyzing the stable aggregate size before and after some energy input. Other indices are directly computed based on a single aggregate size class, to allow for comparisons between soils of various structures (Le Bissonnais, 1996). Water-dispersible clay can be directly used as an indicator, but can also be combined with water-dispersible silt, and total clay and silt contents (Igwe and Udegbunam, 2008).

The main drawback of using aggregate size distribution and stability as indicators is that the results are highly sensitive to methodological details such as the type of sieving, its duration, oscillation frequency, and loading rate (Almajmaie et al., 2017; Beare and Bruce, 1993; Letey, 1991) and that a large number of different methods are actually used (Díaz-Zorita et al., 2002; Le Bissonnais, 1996; Peng et al., 2015). There is, however, a protocol developed by Le Bissonnais (1996) for assessing the stability of soil aggregates subjected to the action of water, which led to an international standard (ISO 10930, 2012). Other important aspects are the

sample pretreatments aiming at homogenizing the water contents (e.g., air-dried samples or rewetted at a given water potential), since they modify the bonding forces (Almajmaie et al., 2017; Beare and Bruce, 1993; Haynes, 1993). Similarly, water-dispersible clay measurement proved to be highly sensitive to pretreatments (i.e., initial water content and wetting rate) and to the amount of energy applied for the dispersion (Czyż and Dexter, 2015; Kjaergaard et al., 2004). So, the results of the different dry and wet sieving protocols were not always consistent, and their ability to discriminate management practices, soil properties, or measured soil loss varied greatly (Le Bissonnais, 1996; Pulido Moncada et al., 2013). Another aspect is that the mechanical work applied during dry sieving is rarely experienced in the field and cannot be easily quantified (Díaz-Zorita et al., 2002). In the same way, the positive pore water pressures applied during wet sieving rarely occur under natural conditions.

Significant correlations between the aggregate size and macroporosity, number of pores, and pore size were observed (Mangalassery et al., 2013). According to Dexter (1988), there is an optimal aggregate size for seed germination between 1 and 5 mm in diameter (physical support function). Aggregate size was also observed to influence the emissions of CO₂, N₂O, and CH₄ (Drury et al., 2004; Mangalassery et al., 2013). However, the existence and direction of the relationships depended on soil texture and SOM content (Mangalassery et al., 2013). Soil aggregation further regulates the capacity of soils to store carbon by physical protection of SOM from microbial and enzymatic attack. The protective capacity of aggregates is mainly related to a spatial separation of substrate and microorganisms as well as to a reduced microbial activity due to a reduced diffusion of oxygen into aggregates (Six et al., 2002). Evidence was found that stable microaggregates play a decisive role for the long-term stabilization of SOM, whereas less stable macroaggregates provide only a minimum of physical protection (Krull et al., 2003; Six et al., 2004, 2002). In this regard, silt-sized microaggregates seem to be of particular importance for carbon storage in both topsoils and subsoils (Han et al., 2015; Moni et al., 2010; Virto et al., 2008). As a measureable indicator, microaggregates-within-macroaggregates were proposed as diagnostic fraction for the carbon sequestration potential in agroecosystems and for soil organic carbon changes induced by management and land use changes in a wide range of soil types and environments (Denef et al., 2007, 2004; Kong et al., 2005; Six and Paustian, 2014).

Aggregate stability appeared to be significant for the susceptibility to erosion of soils. Many authors reported that reduced aggregate stability increases soil susceptibility to runoff, interrill erosion, and crusting (Barthès and Roose, 2002; Nciizah and Wakindiki, 2015). Crusting is

often associated with a reduction of soil aeration and soil permeability. Therefore, aggregate stability and water-dispersible clay are related to the physical stability and support for plants and to the partitioning of water between infiltration and runoff. In addition, since the clay fraction can transport adsorbed nutrients or contaminants along the soil surface with runoff, or downward in the soil profile with infiltrating water (Calero et al., 2008; Czyż and Dexter, 2015), there is a link with the functions of soils for nutrient cycling and for filtering water.

3. Characterization of the pore space

Some laboratory and imaging techniques were designed to characterize the pore space. Given the typical sample sizes of centimeters to decimeters (Figure 2), these methods mainly characterize the “microstructure” (Baize et al., 2013).

3.1. Indirect methods

Indirect methods use probe molecules to derive information about the pore size, volume, and/or pore-solid surface area. As opposed to imaging techniques, these methods are not spatially resolved and do not characterize the morphology and topology of the pore space.

3.1.1. Mercury porosimetry

Mercury porosimetry is a routine method used for decades for the characterization of the pore size distribution. The main reason for its wide use probably lies in the large range of pore sizes that can be investigated in a single run: usually five orders of magnitude, from about 3 nm to 500 μm . A mercury porosimetry analysis is completed within a few hours on soil aggregates between about 2 to 6 cm^3 in size. Instruments are easily available and the repeatability of the method is good. According to Giesche (2006), the standard deviations of pore size and pore volume are $< 1\%$.

Usually, mercury porosimetry is performed in its “intrusion” mode (MIP). As a non-wetting fluid, mercury is forced to intrude a soil sample by applying known increasing pressures, to fill pores of decreasing sizes (Van Brakel et al., 1981). Finally, the volume of intruded mercury as function of the applied pressure is obtained. Pressures are converted into equivalent pore diameters according to the Young-Laplace law, assuming non-connected cylindrical pores, to retrieve the pore size distribution. This equation gives the equivalent pore diameter as function of the pressure, contact angle, and surface tension of mercury. Although rarely done in soil science, mercury porosimetry can also be performed in the “extrusion” mode, by decreasing the

applied pressure (e.g., Jozefaciuk et al., 2015; Otalvaro et al., 2016). A hysteresis is typically found between intrusion and extrusion: mercury can be entrapped in the soil pore space, because of the ink-bottle effect and different contact angles between advancing and receding menisci (Kloubek, 1981). Jozefaciuk et al. (2015) found, for example, differences from 2.4 to 3.5% in pore volume at equivalent capillary pressures between the intrusion and extrusion curves.

Several drawbacks are known to affect MIP, impeding a clear interpretation of the results (Van Brakel et al., 1981). Indeed, in the case of an “ink-bottle” pore, MIP does not measure the actual pore size, but the largest entrance pressure towards this pore, i.e., the neck, and then assumes cylindrical pores when applying the Young-Laplace law to convert pressures into pore diameters (Giesche, 2006). Therefore, pore sizes measured by MIP are always smaller than those measured by imaging methods (Bruand and Cousin, 1995; Giesche, 2006). Even though this is a well-known effect, it is often omitted when interpreting MIP data, assuming that all the compared samples are affected in the same manner. Only a few studies really discussed their results taking into account the ink-bottle effect (e.g., Bruand and Cousin, 1995; Richard et al., 2001). In addition, MIP cannot give information on pores disconnected from the external surface of the investigated aggregate. The derived total porosity is thus underestimated. Another source of error lies in the assumption of a fixed contact angle, usually 130 or 140°, whereas the contact angle is supposed to vary depending on surface roughness, pore geometry, mineralogy, and whether the meniscus is advancing or receding (Kloubek, 1981).

Soil samples need to be first dried otherwise the remaining water would impede mercury intrusion. This drying step is critical for materials with swelling and shrinking properties due to changes in pore geometry and particle rearrangement. Diverse drying techniques exist (e.g., Bruand and Cousin, 1995; Cuisinier and Laloui, 2004; Delage and Pellerin, 1984; Pagliai et al., 2004; Paz Ferreiro et al., 2010), but when compared, they led to different porosities and pore size distributions (Cuisinier and Laloui, 2004; Thompson et al., 1985), so none of them can be considered as a standard. Moreover, there are dissenting opinions regarding the possible modification of soil structure during the process of mercury intrusion (Kozak et al., 1991; Lawrence, 1978), which appeared to be more critical for organic soils (Echeverría et al., 1999).

MIP was used to study soil compaction, which was found to mainly affect macroporosity (Destain et al., 2016). Since the size of pore necks rather than the size of pores controls the movement of organisms in soil, MIP appears also suitable for studying the habitat for biological activity function (Elliott and Coleman, 1988). Given that mercury is a non-wetting fluid, the mercury intrusion process is equivalent to air intrusion during water desorption. Therefore, at

low pressures, the volume of pores not intruded by mercury could be used to deduce the volume of water held at a given matric potential, i.e., the water retention curve (Romero and Simms, 2008). However, discrepancies were observed (Otalvaro et al., 2016; Ragab et al., 1982). They may be due to the distinct soil volumes investigated, typically bigger for the water retention curve determination, leading to different accessibility of pores, and to a modification of soil structure (swelling-shrinking) during the water retention curve determination or the drying of soil samples (Romero and Simms, 2008).

3.1.2. Water retention curve and derived indicators

The pore size distribution can also be derived from the water retention curve, i.e., the relation between soil water content (θ) and matric potential (ψ), using water as the probe molecule (Dexter, 1988; Nimmo, 2005). To do so, the measured water retention curve $\theta = f(\psi)$ needs to be first converted into an equivalent $\theta = f(d)$ curve, with d the maximum water-filled pore diameter, according to the Young-Laplace law and assuming a parallel bundle of cylindrical pores. The derivative of this curve provides an estimation of an “equivalent” pore size distribution (Nimmo, 2005), with the same restriction as for MIP.

Several methods are available to measure the water retention curve, depending on the sample size and the range of matric potential investigated (Dane and Hopmans, 2002). They mainly differ in the way water is extracted, i.e., hanging water column, suction table, pressure plate extractor, or evaporation method. These traditional methods are however prone to error in the dry range, and can thus be complemented by methods based on relative humidity or osmotic equilibration. At tensions close to zero there may be artifacts related to the height of the soil sample (Peters and Durner, 2006). The time required for measuring a water retention curve is usually much longer than for MIP, because of the longer equilibration times. Sample sizes range from a few centimeter clods to cylinders of a few decimeters in diameter. As with MIP, water retention curves are typically hysteretic with separated wetting and drying paths (Dane and Hopmans, 2002). Before converting experimental points into a pore size distribution, a model is adjusted (see Kosugi et al., 2002 for a description of these models). This additional step allows an interpolation between experimental points, but can also introduce errors in the estimation of the pore size distribution in case of a poor fitting quality. It is also worth noting that a considerable number of pedotransfer functions exists, to estimate the water retention curve from basic soil properties, e.g., texture, BD, and SOM content, as reviewed by Vereecken et al. (2010).

The macropore, mesopore, or micropore volumes can be estimated from defined points on the water retention curve (e.g., Kuncoro et al., 2014; Regelink et al., 2015; Reynolds et al., 2009). These points depend on the chosen size limits for the pore size classes, for which there are no generally agreed upon limits. They are calculated from the matric potential and the Young-Laplace equation. To characterize the pore size distribution, location descriptors such as the mode, median and mean, and shape descriptors such as skewness (asymmetry) and kurtosis (peakedness) were used (Pulido Moncada et al., 2014a; Reynolds et al., 2009). According to Pulido Moncada et al. (2014a), location descriptors providing information on the modal, median, or mean pore size are more informative. Reynolds et al. (2009) proposed an optimal pore structure characterized by a large standard deviation of equivalent pore diameters, a substantial skew towards small pore diameters, and modal pore diameters between 60 and 140 μm .

The water retention curve can be used to derive a variety of additional indicators, without any transformation into pore size distribution (Figure 3). Saturated water content equals total porosity when the soil is fully saturated (without entrapped air). Air capacity is defined as the volume of air measured when the soil is at field capacity (e.g., Pulido Moncada et al., 2014c; Reynolds et al., 2009). It is used to characterize aeration for plant roots. The relative field capacity corresponds to the water content at field capacity, divided by the saturated water content, and represents the ability of soils to store water and air (e.g., Pulido Moncada et al., 2013; Reynolds et al., 2009). The hypothesis is that soils with relative field capacity between 0.6 and 0.7 are likely to have desirable water and air contents for long time periods, which is favorable for nitrogen cycling by microorganisms and plants (Reynolds et al., 2009). The available water capacity is the ability of soils to store and provide water available to plant roots, measured as the amount of water held between field capacity and permanent wilting point (e.g., Pulido Moncada et al., 2013; Reynolds et al., 2009). Field capacity is, however, a concept not well defined, and is usually measured at matric potentials of 100 or 330 hPa. This choice was discussed to depend on soil texture (e.g., Zacharias and Bohne, 2008).

Macropore volume, air capacity, relative field capacity, and available water capacity were deemed to be suitable to discriminate soils of “good” and “poor” physical quality for crop production (Reynolds et al., 2009): non-optimal soils showed poor aeration capacity (excessive water retention) or insufficient capacity to store water available for plants. Air capacity and available water capacity also demonstrated a good sensitivity to management practices (Moebius et al., 2007; Pulido Moncada et al., 2014c). Considering the macropore volume, it

was often observed to be affected by compaction, whereas the micropore volume remained unaffected (Kuncoro et al., 2014). As already mentioned for MIP, the pore neck size is probably more useful to describe the movement of organisms in soil than the pore diameter (Elliott and Coleman, 1988). So, by using water retention curves, pore neck sizes were well correlated to the bacterial biomass and diversity and nematode biomass (Hassink et al., 1993; Ruamps et al., 2011). Such good correlations were not observed for fungi and protozoa, because they are able to prospect a large range of pore diameters.

The concept of least limiting water range (LLWR), introduced by da Silva et al. (1994) as an index of soil structural quality, goes beyond the definition of available water capacity. In order to characterize the crop production function, LLWR was defined as the range of water contents within which limitations for plant growth associated with water potential, aeration, and mechanical resistance are minimal (da Silva et al., 1994). To determine the critical limit towards the dry range, water content at permanent wilting point and penetration resistance are taken into account. The critical limit towards the wet range is obtained from water content at field capacity and air capacity (Figure 4). These critical limits are usually obtained from the literature (e.g., Asgarzadeh et al., 2010; Kaufmann et al., 2010). To simplify the determination of LLWR, pedotransfer functions were developed to predict LLWR from BD, clay, SOM contents, and cementing agents (da Silva and Kay, 1997; Neyshabouri et al., 2014). It is possible to find a large number of studies using LLWR to examine the effect of different management practices or land uses. However, De Jong van Lier and Gubiani (2015) stated that LLWR does not include the current knowledge of the physical and biological processes occurring during crop growth, so that LLWR did not prove to be efficient to explain crop yields. These authors argued that the wet and dry critical limits are often chosen to be fixed values, whereas these limits are functions of time, depth, soil type, and plant physiology.

The S index developed by Dexter (2004a) is another indicator derived from the water retention curve, intending to represent soil physical quality. It is calculated as the slope of the water retention curve $W = f(\ln |\psi|)$ at its inflection point (with W , the gravimetric water content). By definition, the peak of the pore size distribution derived from the water retention curve corresponds to the slope at the inflection point (Reynolds et al., 2009). Thus, the S-theory implicitly assumes a unimodal distribution of the pore sizes. For a van Genuchten (1980) parametrization, the S index is directly related to the parameter n (de Jong van Lier, 2014). The postulate of Dexter (2004a) is that the presence of structural pores is essential for soil physical quality, and that textural porosity is little affected by soil management contrary to structural

porosity. The value of S is indicative of the extent to which the soil porosity is concentrated into a narrow range of pore sizes (Dexter, 2004a). A low S index corresponds to a structureless soil, whereas a high S index corresponds to a structured soil with pores of different sizes (Dexter, 2004a). A threshold of $S = 0.035$ was suggested to distinguish “good” and “poor” soil physical qualities (Dexter, 2004a). An exception appears for sands, for which the S index may be poorly adapted, because of a lack of structural pores (Reynolds et al., 2009).

The S index was observed to be positively correlated with root development (except for sands) (Dexter, 2004a; Kaufmann et al., 2010), soil friability (Dexter, 2004b), and unsaturated hydraulic conductivity at the inflection point (Dexter, 2004c). Some relationships with other indicators of soil structure were investigated. Correlations were observed with BD (Dexter, 2004a), packing density and LLWR (Asgarzadeh et al., 2010; Kaufmann et al., 2010), relative field capacity, available water capacity, air capacity, macroporosity, structural stability index (Reynolds et al., 2009), and degree of compactness (Naderi-Boldaji and Keller, 2016).

3.1.3. Gas adsorption

Like MIP and the water retention curve, physical gas adsorption methods are indirect methods, using probe molecules to derive properties of the soil pore space in the form of adsorption isotherms (Zachara et al., 2016). Since physical adsorption is involved, all surface sites accessible to the probe molecules are theoretically investigated, as opposed to chemical adsorption (Heister, 2014). In soil science applications, adsorptives are mainly dinitrogen (N_2) (e.g., Hall et al., 2013; Zong et al., 2015), CO_2 (e.g., Echeverría et al., 1999; Ravikovitch et al., 2005), and water vapor (e.g., Jozefaciuk et al., 2015). When using N_2 , the analysis is performed at 77 K ($-196^\circ C$). For CO_2 , experiments are performed at 273 K ($0^\circ C$) and for water at 293 K ($20^\circ C$). The analysis is carried out on small soil samples, about 1 to 5 mm in diameter, and the pore size investigated usually ranges between 1 and 200 nm. Thus, gas adsorption addresses the lower spatial limit for the characterization of soil structure. The required instruments are easily available. However, due to the limitation to very small pore sizes this method is only relevant for some specific studies. In addition, considering this fine spatial resolution, users usually adopt the pore size terminology given by the IUPAC (Sing et al., 2008), rather than the terminology used in soil science: macropores are defined as pores with diameters > 50 nm, mesopore diameters are in the range of 2–50 nm, and micropore diameters are < 2 nm. We will follow this classification in the current section. The reproducibility of the method is recognized to be good (Jozefaciuk et al., 2015; Mayer et al., 2004). For example, by using water desorption isotherms, Jozefaciuk et al. (2015) observed differences $< 1.7\%$ between isotherms measured

in triplicate. Eusterhues et al. (2005) found standard deviations in the range of 2–10% when comparing several N₂ adsorption measurements of the same sample.

Prior to the analysis, samples are degassed (under vacuum or with a flowing gas, and heated) to remove adsorbed molecules including water vapor (Sing et al., 2008), e.g., 1 h at 200°C in Séquaris et al. (2010), 150°C overnight in Mayer et al. (2004), 24 h at 120°C in Ravikovitch et al. (2005). Then, the relative pressure p/p^0 is increased in the measurement cell (where p is the partial pressure of the adsorptive and p^0 is its equilibrium vapor pressure at the temperature of the measurement). The quantity of adsorbed gas is calculated from the difference of pressure before and after the establishment of equilibrium, or by weighing in the case of water adsorption (Sing et al., 2008). The relative pressure is then increased by known increments at constant temperature. During these steps, monolayer, then multilayer adsorption occurs. Micropores are filled first, because of high interactions between the adsorbate and the pore walls (Lowell et al., 2004). Then, during mesopore and macropore filling, adsorption does not only depend on interaction with pore walls, but also on attractive interaction between adsorbates themselves (Lowell et al., 2004). In this case, the space remaining at the center of the pores after multilayer adsorption on their walls is filled. This mechanism is denoted as capillary condensation, i.e., the gas phase condenses to fill pores at a pressure lower than its saturation pressure, a meniscus is formed at the interface with the vapor phase, and the fluid filling the pore is considered as a liquid (Lowell et al., 2004; Sing et al., 2008). Then, desorption curve is obtained by decreasing the relative pressure.

The specific surface area is often calculated from the Brunauer-Emmett-Teller model (BET, Brunauer et al., 1938), for a relative pressure ranging between 0.05 and 0.30 (e.g., Hall et al., 2013; Ravikovitch et al., 2005; Zong et al., 2015). It predicts the number of molecules required to form a monolayer on the sample surface. The total pore volume and the mean pore diameter can then be deduced using data close to saturation (e.g., Séquaris et al., 2010). Among other methods, the Barrett-Joyner-Halenda theory (BJH, Barrett et al., 1951) can be used to determine the mesopore volume and the pore size distribution in the mesopore range (e.g., Zong et al., 2015). The t-plot method (de Boer et al., 1966) can be used to estimate the micropore volume and surface area from N₂ isotherms. The shape of the hysteresis loop formed by the adsorption and desorption paths allows further interpretation of the pore shapes (Sing et al., 2008). Like all indirect methods, several hypotheses need to be presumed for a valid interpretation, among others, the domain of validity in terms of pore sizes and an idealized pore shape (Zachara et al., 2016).

Gas adsorption protocols require heating the soil samples. Heating aims at promoting evaporation, but can cause phase changes in some oxides and hydroxides, a loss of water in the interlayers of clay minerals, and presumably a structural reorganization of SOM, as reported in the review of Heister (2014). To prevent changes in oxides and hydroxides, Kaiser and Guggenberger (2003) degassed their air-dried samples at 20°C during 48 h. Moreover, N₂ proved to be inadequate to characterize soils with high amounts of SOM, contrary to CO₂ (Echeverría et al., 1999; Ravikovitch et al., 2005). According to de Jonge and Mittelmeijer-Hazeleger (1996), the surface area of SOM measured with N₂ gas adsorption might be underestimated by two orders of magnitude. This is linked to the slow diffusion of N₂ at 77 K, which restricts its adsorption in small pores of SOM (de Jonge and Mittelmeijer-Hazeleger, 1996; Echeverría et al., 1999; Ravikovitch et al., 2005). In addition, differences were observed between water desorption and N₂ adsorption methods, and explained by the effect of polar water molecules and a modification of the pore structure by the addition of water (Hajnos et al., 2006). A larger specific surface area theoretically provides more reactive sites and thus more possibilities for a substance to interact with the soil solid phase (Heister, 2014). In particular, a correlation was sometimes found between SOM content and specific surface area measured with N₂ adsorption, after SOM destruction (e.g., Kaiser and Guggenberger, 2003; Séquaris et al., 2010). This correlation may be related to the preferential association of SOM with clay particle edges and oxyhydroxides (Kaiser and Guggenberger, 2003; Mayer et al., 2004). However, because SOM adsorption occurs at specific reactive sites, i.e., in patches rather than as a continuous coating (Kaiser and Guggenberger, 2003), this relationship may be too weak to correlate specific surface area to the carbon storage function. For the same reason, micropore and mesopore volumes measured with N₂ adsorption cannot be interpreted as reliable indicators of carbon storage either (Eusterhues et al., 2005; Mayer et al., 2004). The pore sizes resolved with gas adsorption are so small that the majority of the surface area is unavailable for microbial colonization (Darbyshire et al., 1993) and water is only extracted from pores in the investigated size range at pF > 4.2.

3.2. Direct methods

Imaging techniques are considered here as direct methods, since they allow for the evaluation of the soil pore space by direct geometric visualization. Thin sections and serial sections observed by optical microscopes have been used for decades to provide 2-D and 3-D representations of the soil pore network (e.g., Pagliai et al., 2004; Skvortsova and Sanzharova,

2007). Next to optical microscopy, scanning electron microscopy (SEM) in backscattered electron mode can be used for structural analyses (e.g., Bruand and Cousin, 1995; Richard et al., 2001). This method requires sample preparation in thin sections. Other methods use radiations interacting with the atoms constituting soil, with the advantage of being non-destructive for soil structure. Examples are X-ray tomography (Cnudde and Boone, 2013; Wildenschild and Sheppard, 2013), gamma-ray tomography (e.g., Pires et al., 2005), neutron tomography (e.g., Schaap et al., 2008; Tumlinson et al., 2008), and nuclear magnetic resonance imaging (e.g., Pohlmeier et al., 2008; Sněhota et al., 2010). The latter two methods are rather efficient to image the water phase.

Stereological methods are used to retrieve 3-D information from 2-D images or descriptors are calculated directly from reconstructed 3-D images. In any case, images always need to be processed and optimized for subsequent quantitative analysis. A preprocessing step often consists in applying spatial registration, noise and/or artifact removal, or edge enhancement, as reviewed by Schlüter et al. (2014) and Tuller et al. (2013). Then, if contrast is satisfactory, the segmentation step allows distinguishing different phases as air, water, soil matrix, roots, or gravels. Matrix is here defined as the solid phase including pores (water- and air-filled) with a size lower than the image resolution. The size of the soil sample usually depends on the resolution to be achieved and on the imaging technique used (Wildenschild et al., 2002): resolution can range, for example, from about hundred micrometers using a medical X-ray scanner on a decimeter sample, to a few micrometers using synchrotron-based X-ray tomography on a few millimeter samples. Generally, the ratio between voxel size and sample size is constrained by the properties of the detector panel and ranges between 500 and 2000.

First, images can be described visually in a qualitative way, by classifying voids with a typology based on their origin, e.g., biogenic pores, cracks, or textural voids (Skvortsova and Utkaeva, 2008). But the strength of imaging techniques rather lies in the plethora of quantitative morphological and topological descriptors which can be extracted from the images (Helliwell et al., 2013). In contrast to the indirect methods to characterize the soil pore space (Section 3.1), meaningful measures such as porosity, pore size distribution, and interfacial area can be retrieved directly, without any assumptions on the pore shape. Some other basic descriptors are the number, length, shape, and orientation of pores (Horgan, 1998; Skvortsova and Utkaeva, 2008). These descriptors are often highly correlated. Some other descriptors characterize the tortuosity, connectivity, or percolation threshold (Jarvis et al., 2017; Renard and Allard, 2013; Vogel et al., 2010). When considering the percolation of the air-phase, the percolation threshold

is defined as the lowest porosity at which two opposite faces of the sample are connected by a continuous path. Below this threshold, transport in the air-phase is limited. More complex indicators can be computed to distinguish geometric shape classes of soil pores, from fissure-like to rounded pores (Skvortsova and Sanzharova, 2007), or the distance from any point of the water-filled soil matrix to the closest air-filled pore (Schlüter and Vogel, 2016). This latter indicator can be used to estimate the diffusion length of oxygen, which provides essential information on the redox conditions for microbial activity. All of these descriptors can be calculated on the total pore network, on pores connected to soil surface, or on isolated pores (e.g., Garbout et al., 2013), and in several directions to observe the presence of potential gradients (e.g., Katuwal et al., 2015; Schlüter and Vogel, 2016). By repeating the calculation of a given descriptor on volumes of increasing sizes, it is also possible to evaluate the representative elementary volume of a given descriptor (e.g., Baveye et al., 2002; Costanza-Robinson et al., 2011; Vogel et al., 2002). This can only be performed through non-destructive imaging techniques.

However, imaging techniques require expensive instrumentations, expertise, and computing power for image analyses. The segmentation step is particularly sensitive to subjective errors, and its quality directly affects the calculated metrics (Schlüter et al., 2014; Tuller et al., 2013). Various segmentation methods are available, from fully automated to completely operator-dependent. They can lead to very different segmented images, depending on both the method and operator (Baveye et al., 2010). This lack of standard protocol limits comparisons between studies (Helliwell et al., 2013), but no method appears ideal to be applied to a wide range of porous media (Tuller et al., 2013). The segmentation step is especially hindered by noise and partial volume effects, i.e., a blur at object boundaries where average values of different objects are observed. Lehmann et al. (2006), using sand and glass beads, demonstrated that partial volume effects only disappear when the image resolution is $< 10\%$ of the mean particle size. Vogel et al. (2010) showed that the uncertainty in quantifying soil structure increases significantly when structural units smaller than about 5 pixels in diameter are interpreted. Once this small-scale information is excluded, image segmentation is far less critical. In the same way, quantifying objects bigger than half of the image size should be avoided, because they are not captured in a representative way (Horgan, 1998).

Because the soil pore geometry was observed to be more sensitive to changes in management practices than some bulk measurements like BD (Skvortsova and Utkaeva, 2008), imaging techniques are attractive tools to assess soil functions. A first set of indicators is related to the

pore shape and orientation. As an example, the presence of elongated pores and their orientation were related to water movement and leaching processes (Pagliai and Vignozzi, 2002; Skvortsova and Utkaeva, 2008). Pore orientation and elongation were also observed to be sensitive to management practices, such as tillage or amendment application (Pagliai et al., 2004).

According to Dal Ferro et al. (2012) and Zong et al. (2015), imaging techniques provide a measure of the pore size distribution which is closer to reality than MIP in the overlapping range of pore sizes, because they are not affected by the ink-bottle effect and do not modify soil structure. However, taking into account the ink-bottle effect may be suitable for the soil function related to water retention and transport. Correlations between macroporosity and air permeability, gas diffusivity, and water transport including preferential flow were found (Katuwal et al., 2015; Larsbo et al., 2014; Naveed et al., 2014b; Paradelo et al., 2016). In the study of Luo et al. (2010), for example, macroporosity explained a greater proportion of variability in saturated hydraulic conductivity than BD. There are also experimental evidences that pores of medium size (in the range ~30–90 μm) might play an important role in carbon loss, because of the conditions of air, water, and nutrient supply they provide for OM decomposition (Ananyeva et al., 2013; Kravchenko et al., 2015; Strong et al., 2004; Toosi et al., 2017). Conversely, small pores may provide a physical protection for OM. As a feedback mechanism, carbon sequestration was observed to increase the volume of mesopores and micropores, therefore reducing the risk of fast transport and leaching in macropores (Larsbo et al., 2016). Porosity and pore size distribution were often observed to be affected by management practices such as tillage, amendment application, crop rotation, or land use (Munkholm et al., 2016; Naveed et al., 2014a; Schlüter et al., 2011).

Connectivity of the pore network is also a key parameter for soil biota including plant growth as well as for water and gas transport. Connectivity appeared to drive saturated hydraulic conductivity (Luo et al., 2010; Sandin et al., 2017), air permeability (Paradelo et al., 2016), and the release of greenhouse gases (Rabot et al., 2015). In addition, several studies showed that particulate organic matter decomposition was affected by pore characteristics. Indeed, the accessibility for organisms and aeration status were controlled by the pore connectivity to the atmosphere and the pore size (Kravchenko et al., 2015; Negassa et al., 2015; Rabbi et al., 2016). The pore connectivity parameter was observed to be sensitive to tillage, fertilization, and land use (Dal Ferro et al., 2014; Jarvis et al., 2017; Naveed et al., 2014a; Schlüter et al., 2011). However, connectivity estimated through the Euler number was not always considered a good

measure of macropore connectivity (Katuwal et al., 2015). Indeed, this metric is highly affected by isolated voxels, like unconnected structural pores and thresholding artifacts (Renard and Allard, 2013). Connectivity can also be quantified with the genus density, which only considers the number of loops or redundant connections used to compute the Euler number (e.g., Paradelo et al., 2016) or the path number, i.e., the number of independent and continuous paths between two boundaries (e.g., Luo et al., 2010). Additional measures of connectivity are based on the percolating network, with high significance for preferential flow and transport processes (Jarvis et al., 2017; Sandin et al., 2017). Jarvis et al. (2017) calculated the percolating pore space (i.e., the volume of pores connected to both the top and bottom of the sample) and the proportion of the pore volume represented by the largest cluster. A cluster is here defined as a group of connected pore voxels. The connection probability or Γ connectivity is the second moment of the cluster size distribution (Jarvis et al., 2017; Renard and Allard, 2013; Schlüter and Vogel, 2016), and equals the square of the percolating pore fraction. It represents the probability that two randomly chosen pore voxels belong to the same cluster (Jarvis et al., 2017). So, Γ connectivity indicates the probability for a connected pathway to exist, whereas the Euler number indicates how many connected pathways exist (Herring et al., 2015).

It is noteworthy that some imaging techniques were recently developed to be used directly in the field, e.g., the method used by Eck et al. (2016) based on laser triangulation, to extract macropores on a dry soil profile. After correcting the pore widths from a swelling effect, Eck et al. (2016) found a significant correlation with the saturated hydraulic conductivity. This example highlights that scanning at the soil horizon or soil profile scale is relevant to characterize water transfers. There would be a priori no major difference linked to the resolution as compared to a coarse-resolution X-ray scanner and the measurement area is similar to that of a visual profile description. However, a major drawback of this technique is that it only provides a 2-D characterization and not a 3-D characterization like tomographic imaging methods do.

4. Discussion

4.1. Solid phase vs. pore space perspective

Characterizing soil structure from the perspective of aggregates has been criticized (Baveye, 2006; Letey, 1991; Pagliai and Vignozzi, 2002; Young et al., 2001). Although appealing, the aggregate perspective does not seem to be the most appropriate to link soil structure with soil functions and processes. The main reason is that analyzing aggregates is more related to the

mechanical stability of soil structure rather than to the structure itself. Of course, stability is an important feature but soil processes acting within a given soil are sensitive to the morphological structure of pores and solid which cannot be addressed based on aggregates. Another reason is methodological. As stated above, aggregate size and stability measurements highly depend on the energy applied. Therefore, results may depend on the measurement method used, rather than on soil structure (Young et al., 2001). Moreover, and more general, Young et al. (2001) questioned the existence of distinct soil aggregates in an undisturbed soil profile. They asserted that aggregates are just the result of how we choose to observe them, by applying a given energy.

From that, Baveye (2006), Letey (1991), Pagliai and Vignozzi (2002), and Young et al. (2001) suggested characterizing the pore space, rather than a bed of aggregates. Processes occurring in soil are controlled by the pore shape, pore size distribution, pore surface density, connectivity, tortuosity, and heterogeneity of the pore space in three-dimensions (Pagliai and Vignozzi, 2002; Young et al., 2001). They directly influence storage and movement of water, solutes and gases, and root development (Pagliai and Vignozzi, 2002). Moreover, the pore space perspective offers a continuous analysis of the processes occurring in soils, conveniently managed by models, contrary to the discrete analysis proposed by the aggregate perspective. Morphological characteristics based on undisturbed samples could be the key to incorporate quantitative information on soil structure into models (Kravchenko and Guber, 2017).

In Figure 5, we compare the result of the manual generation of aggregates of four soil samples varying in texture and land use, as could be done during a field description of soil structure, with cross-section images of undisturbed soil samples obtained with X-ray computed tomography. We carefully broke apart dry clods by hand, then put the resulting fragments on a piece of paper illuminated from the bottom with a LED light panel. Most of the aggregates produced were subangular and their size depended on the energy applied. On the contrary, huge differences are evident between the four soil samples in the X-ray images, in terms of pore shape formed by microcracks, packing voids, root channels, and earthworm burrows with visible porosity (pores $> 20 \mu\text{m}$ in diameter) in the range of 10–16% and vastly different pore size distributions (data not shown). Moreover the soils appear to differ regarding the heterogeneity in the soil matrix, i.e., visible aggregates in the Kühnfeld soil (a), sand in a fine-textured matrix in the Hadera soil (b), and fine-textured loess in the Bad Lauchstädt (c) and Garzweiler soils (d). These examples highlight the fact that soil structure can be addressed much

more precisely by using undisturbed soil samples. Moreover, these two approaches investigate distinct scales, thus leading to different visible features.

4.2. Comparison between indicators

Methods commonly used for soil structure characterization mainly aim at estimating the soil compactness, aggregate shape, grade, size and stability, or pore network morphology and topology. Their known advantages and limitations are reported in Table 1. Field evaluations of soil structure, based on the fundamental principles of soil surveys, provide valuable information about soil structure. Some of them are fast and cheap, but have the disadvantage of being semi-quantitative and of requiring a trained eye. Measuring the aggregate size distribution and stability is labor-intensive, and suffers from a lack of standard in the sample pretreatment and in the measurement itself. Despite these drawbacks, the use of aggregate size distribution and stability tests is highly valuable in erosion studies. BD is not considered to be a good indicator for soil functions in general, because it does not take into account important soil structural attributes. Indirect methods to characterize the pore space, such as the water retention curve, MIP, and gas adsorption, all require assumptions on an idealized pore shape to interpret the results. Using an assumption on the pore shape to characterize the pore shape is, of course, a questionable approach. Moreover, the water retention curve and MIP are both subject to the ink-bottle effect, a well-known phenomenon not always taken into consideration when interpreting the results. However, because of the implicit consideration of the ink-bottle effect, they might be suitable for studying soil functions related to water retention and transport. In fact, the concept of Mualem (1976) to derive the relative hydraulic conductivity based on the water retention curve is pretty successful, probably because it implicitly includes the ink-bottle effect (Vogel, 2000). Finally, laboratory-based imaging techniques appear to be efficient in characterizing soil structure because they not only allow quantifying the pore volume, pore size distribution, and interfacial area, but also the pore connectivity and pore contact distances, with an additional significance for soil functions. Since these indicators are spatially resolved, the presence of gradients can be studied and calculations can be restricted to a given group of pores relevant for the soil function under consideration (e.g., connected to soil surface). Imaging techniques used in the field are promising since they allow scanning large areas, but they only provide a 2-D characterization of a soil profile.

Throughout this review, we gathered evidences that soil moisture conditions could be an obstacle to evaluate and compare a given indicator at any period of the year. Indeed, a

significant modification of soil structure is often observed after wetting and after drying a soil sample, because of swelling and shrinking phenomena (Della Vecchia et al., 2015; Simms and Yanful, 2001). This highlights the dependency of the pore size distribution to the soil water content. To address this problem, aggregate size distribution and aggregate stability tests often use dry or rewetted soil samples to establish standard conditions of soil moisture and hydric history, but with possible damaging effects on soil structure (Dexter, 1988). Eck et al. (2016) normalized the pore diameters measured under dry conditions by the coefficient of linear extensibility, to retrieve the macropore diameters that would be measured at saturation. MIP and gas adsorption methods also use dry samples. With respect to pore space morphology, however, none of these methods appears actually able to provide reliable information using a single measurement.

Some of these methods are themselves sensitive to soil texture or SOM content because they require the breakdown of aggregates. Additionally, a given bulk density would not be interpreted the same way in a sandy and a clayey soil, because the aggregation of primary particles is extremely different. On the contrary, the metrics derived from imaging are measured independently of the aggregation process and can thus be interpreted directly. For these reasons, to use soil structure as an efficient indicator of soil functions, it is necessary to characterize the pore space of undisturbed soil samples.

The indicators presented in this review are evaluated according to their relevance to the investigated soil functions in Table 2. Unsurprisingly, several indicators of soil structure are able to characterize the function related to the storage and filtering of water. The habitat for biological activity function appeared to be quite conveniently assessed by using indirect methods subject to the ink-bottle effect. On the contrary, the storage and recycling of nutrients and carbon storage functions are more difficult to assess with indicators of soil structure since these functions also involve chemical reactions. However, some indicators controlling water movement and erosion, such as the macroporosity, pore orientation, pore connectivity, and stability index allow for characterizing these two soil functions at least partly. The major difficulty in assessing the biomass production function (i.e., soil fertility) is that critical thresholds of indicators are expected to depend on plant physiology. Finally, the physical stability and support function is mostly assessed through aggregate stability tests. Considering the methodological limitations discussed above, porosity, macroporosity, pore distances, and pore connectivity appear to be the most relevant indicators for several soil functions.

Modeling is another valuable and more integrated approach to assess soil functions. Crop growth models, biogeochemical models, water dynamics, or erosion models do not explicitly claim that they were designed to assess soil functions. However, some of their output variables can be used to assess them. We can cite the example of the crop biomass to assess the biomass production or amount of eroded soil for the physical stability and support function. The modeling approach is often time-consuming and requires very detailed input data (Greiner et al., 2017). However, modeling allows estimating the long-term effect of a future climate, land use, or management practice on soil functions. In such an approach, the soil structural properties described in this review have the potential of being used as key variables of the models.

4.3. A need for a soil structure library

One major conclusion of this review is that pore network characterization based on undisturbed samples is much more powerful to assess soil functions as compared to the analysis of disturbed aggregates. Today, excellent tools exist to quantify soil structure using non-destructive tomographic techniques (mainly X-ray computed tomography). However, these tools are restricted to specialized laboratories and are not widely applicable to characterize field soils. On the other hand, a wide number of field methods and simple laboratory tools are accessible but their applications are highly subjective and many protocols depend on boundary conditions which are hard to control (e.g., actual soil water content). This poses a fundamental dilemma.

Since imaging techniques are not accessible outside of a research context, effort should be made to produce knowledge about structural characteristics for a large range of soil types in connection to their functional characteristics. This will allow for an extended exploration of how soil structure is related to soil functions. As a first step, we suggest developing standardized protocols to quantify soil structure based on undisturbed imaging in terms of pore morphology and topology. In a next step, an open access “soil structure library” could be established, gathering information on the selected indicators together with their metadata (e.g., imaging technique, sampled volume, image resolution), a site and soil characterization (e.g., soil type, texture, SOM content, sampling depth, etc.), and complementary soil properties (e.g., other indicators of soil structure, saturated hydraulic conductivity, air permeability, etc.). Finally, through this database, it will become possible to establish relationships between selected indicators of undisturbed soil structure with simpler indicators of soil structure in a site-specific way. This has, to some extent, the potential to solve the above mentioned dilemma and will be the subject of a forthcoming paper.

5. Conclusion

In this review, we intended to identify relevant indicators of soil structure to assess soil functions. We identified porosity, macroporosity, pore distances, and pore connectivity as relevant for several soil functions. Imaging instruments appeared to be the most reliable tools to measure them. Up to now, imaging techniques demonstrated their efficiencies, essentially to characterize water dynamics, and so the soil function related to water storage and transport of non-reactive substances. New insights also emerged recently for the carbon storage function, recognizing a more important role to the physical protection of SOM. Additional knowledge could be gathered by broadening the questions tackled using imaging techniques, for example about the physical stability and support function. In this review, we did not draw any conclusions about the exact type of relationships between the selected indicators and soil functions, but we reduced considerably the number of soil structural properties to be included in a meta-analysis. We believe that these relationships are typically not linear, thus requiring reviewing a very large amount of studies on different soil types and management practices to span the whole range of these properties and to draw reliable conclusions. Since imaging techniques are not accessible outside of a research context, effort should be made to produce knowledge for a large range of soil types through a “soil structure library”, in order to characterize and derive relationships for soils of similar functioning.

Acknowledgments

This work was funded by the German Federal Ministry of Education and Research (BMBF) in the framework of the funding measure “Soil as a Sustainable Resource for the Bioeconomy – BonaRes”, project “BonaRes (Module B): BonaRes Centre for Soil Research, subprojects A and C” (grants 031A608A and 031A608C).

References

- Ad-hoc-AG Boden, 2005. *Bodenkundliche Kartieranleitung (KA 5)*. Schweizerbart, Stuttgart.
- Almajmaie, A., Hardie, M., Acuna, T., Birch, C., 2017. Evaluation of methods for determining soil aggregate stability. *Soil Tillage Res.* 167, 39–45. doi:10.1016/j.still.2016.11.003
- Ananyeva, K., Wang, W., Smucker, A.J.M., Rivers, M.L., Kravchenko, A.N., 2013. Can intra-aggregate pore structures affect the aggregate’s effectiveness in protecting carbon? *Soil Biol. Biochem.* 57, 868–875. doi:10.1016/j.soilbio.2012.10.019

- Angers, D.A., Recous, S., Aita, C., 1997. Fate of carbon and nitrogen in water-stable aggregates during decomposition of $^{13}\text{C}^{15}\text{N}$ -labelled wheat straw in situ. *Eur. J. Soil Sci.* 48, 295–300. doi:10.1111/j.1365-2389.1997.tb00549.x
- Asgarzadeh, H., Mosaddeghi, M.R., Mahboubi, A.A., Nosrati, A., Dexter, A.R., 2010. Soil water availability for plants as quantified by conventional available water, least limiting water range and integral water capacity. *Plant Soil* 335, 229–244. doi:10.1007/s11104-010-0410-6
- Baize, D., Duval, O., Richard, G., 2013. *Les sols et leurs structures. Observations à différentes échelles.* Editions Quae, Versailles.
- Baize, D., Jabiol, B., 2011. *Guide pour la description des sols, Collection Savoir-Faire.* Editions Quae.
- Ball, B.C., Batey, T., Munkholm, L.J., 2007. Field assessment of soil structural quality - a development of the Peerlkamp test. *Soil Use Manag.* 23, 329–337. doi:10.1111/j.1475-2743.2007.00102.x
- Ball, B.C., Batey, T., Munkholm, L.J., Guimarães, R.M.L., Boizard, H., McKenzie, D.C., Peigné, J., Tormena, C.A., Hargreaves, P., 2015. The numeric visual evaluation of subsoil structure (SubVESS) under agricultural production. *Soil Tillage Res.* 148, 85–96. doi:10.1016/j.still.2014.12.005
- Barrett, E.P., Joyner, L.G., Halenda, P.P., 1951. The determination of pore volume and area distributions in porous substances. I. Computations from nitrogen isotherms. *J. Am. Chem. Soc.* 73, 373–380. doi:10.1021/ja01145a126
- Barthès, B., Roose, E., 2002. Aggregate stability as an indicator of soil susceptibility to runoff and erosion; validation at several levels. *Catena* 47, 133–149. doi:10.1016/S0341-8162(01)00180-1
- Bauer, T., Strauss, P., Murer, E., 2014. A photogrammetric method for calculating soil bulk density. *J. Plant Nutr. Soil Sci.* 177, 496–499. doi:10.1002/jpln.201400010
- Baveye, P., 2006. Comment on “Soil structure and management: A review” by C.J. Bronick and R. Lal. *Geoderma* 134, 231–232. doi:10.1016/j.geoderma.2005.10.003
- Baveye, P., Rogasik, H., Wendroth, O., Onasch, I., Crawford, J.W., 2002. Effect of sampling volume on the measurement of soil physical properties: simulation with x-ray tomography data. *Meas. Sci. Technol.* 13, 775–784. doi:10.1088/0957-0233/13/5/316

- Baveye, P.C., Laba, M., Otten, W., Bouckaert, L., Dello Sterpaio, P., Goswami, R.R., Grinev, D., Houston, A., Hu, Y., Liu, J., Mooney, S., Pajor, R., Sleutel, S., Tarquis, A., Wang, W., Wei, Q., Sezgin, M., 2010. Observer-dependent variability of the thresholding step in the quantitative analysis of soil images and X-ray microtomography data. *Geoderma* 157, 51–63. doi:10.1016/j.geoderma.2010.03.015
- Beare, M.H., Bruce, R.R., 1993. A comparison of methods for measuring water-stable aggregates: implications for determining environmental effects on soil structure. *Geoderma* 56, 87–104. doi:10.1016/0016-7061(93)90102-Q
- Boizard, H., Peigné, J., Sasal, M.C., de Fátima Guimarães, M., Piron, D., Tomis, V., Vian, J.-F., Cadoux, S., Ralisch, R., Tavares Filho, J., Heddadj, D., De Battista, J., Duparque, A., Franchini, J.C., Roger-Estrade, J., 2017. Developments in the “profil cultural” method for an improved assessment of soil structure under no-till. *Soil Tillage Res.* 173, 93–103. doi:10.1016/j.still.2016.07.007
- Bottinelli, N., Jouquet, P., Capowiez, Y., Podwojewski, P., Grimaldi, M., Peng, X., 2015. Why is the influence of soil macrofauna on soil structure only considered by soil ecologists? *Soil Tillage Res.* 146, 118–124. doi:10.1016/j.still.2014.01.007
- Bruand, A., Cousin, I., 1995. Variation of textural porosity of a clay-loam soil during compaction. *Eur. J. Soil Sci.* 46, 377–385. doi:10.1111/j.1365-2389.1995.tb01334.x
- Brubaker, S.C., Holzhey, C.S., Brasher, B.R., 1992. Estimating the water-dispersible clay content of soils. *Soil Sci. Soc. Am. J.* 56, 1226–1232. doi:10.2136/sssaj1992.03615995005600040036x
- Brunauer, S., Emmett, P.H., Teller, E., 1938. Adsorption of gases in multimolecular layers. *J. Am. Chem. Soc.* 60, 309–319. doi:10.1021/ja01269a023
- Calero, N., Barrón, V., Torrent, J., 2008. Water dispersible clay in calcareous soils of southwestern Spain. *Catena* 74, 22–30. doi:10.1016/j.catena.2007.12.007
- Christensen, B.T., 2001. Physical fractionation of soil and structural and functional complexity in organic matter turnover. *Eur. J. Soil Sci.* 52, 345–353. doi:10.1046/j.1365-2389.2001.00417.x
- Cnudde, V., Boone, M.N., 2013. High-resolution X-ray computed tomography in geosciences: A review of the current technology and applications. *Earth-Science Rev.* 123, 1–17. doi:10.1016/j.earscirev.2013.04.003

- Costanza-Robinson, M.S., Estabrook, B.D., Fouhey, D.F., 2011. Representative elementary volume estimation for porosity, moisture saturation, and air-water interfacial areas in unsaturated porous media: Data quality implications. *Water Resour. Res.* 47, 1–12. doi:10.1029/2010WR009655
- Cuisinier, O., Laloui, L., 2004. Fabric evolution during hydromechanical loading of a compacted silt. *Int. J. Numer. Anal. Methods Geomech.* 28, 483–499. doi:10.1002/nag.348
- Czyż, E.A., Dexter, A.R., 2015. Mechanical dispersion of clay from soil into water: readily-dispersed and spontaneously-dispersed clay. *Int. Agrophysics* 29, 1–7. doi:10.1515/intag-2015-0007
- da Silva, A.P., Kay, B.D., 1997. Estimating the Least Limiting Water Range of soils from properties and management. *Soil Sci. Soc. Am. J.* 61, 877–883. doi:10.2136/sssaj1997.03615995006100030023x
- da Silva, A.P., Kay, B.D., Perfect, E., 1997. Management versus inherent soil properties effects on bulk density and relative compaction. *Soil Tillage Res.* 44, 81–93. doi:10.1016/S0167-1987(97)00044-5
- da Silva, A.P., Kay, B.D., Perfect, E., 1994. Characterization of the Least Limiting Water Range of soils. *Soil Sci. Soc. Am. J.* 58, 1775–1781. doi:10.2136/sssaj1994.03615995005800060028x
- Dal Ferro, N., Delmas, P., Duwig, C., Simonetti, G., Morari, F., 2012. Coupling X-ray microtomography and mercury intrusion porosimetry to quantify aggregate structures of a cambisol under different fertilisation treatments. *Soil Tillage Res.* 119, 13–21. doi:10.1016/j.still.2011.12.001
- Dal Ferro, N., Sartori, L., Simonetti, G., Berti, A., Morari, F., 2014. Soil macro- and microstructure as affected by different tillage systems and their effects on maize root growth. *Soil Tillage Res.* 140, 55–65. doi:10.1016/j.still.2014.02.003
- Dane, J.H., Hopmans, J.W., 2002. Water retention and storage, in: Dane, J.H., Topp, G.C. (Eds.), *Methods of Soil Analysis. Part 4. Physical Methods*. Soil Science Society of America, Book Series No. 5, Madison, WI., pp. 671–719.
- Darbyshire, J.F., Chapman, S.J., Cheshire, M. V., Gauld, J.H., McHardy, W.J., Paterson, E., Vaughan, D., 1993. Methods for the study of interrelationships between micro-organisms and soil structure. *Geoderma* 56, 3–23. doi:10.1016/0016-7061(93)90097-5

- de Boer, J.H., Lippens, B.C., Linsen, B.G., Broekhoff, J.C.P., van den Heuvel, A., Osinga, T.J., 1966. The t-curve of multimolecular N₂-adsorption. *J. Colloid Interface Sci.* 21, 405–414. doi:10.1016/0095-8522(66)90006-7
- de Jong van Lier, Q., 2014. Revisiting the S-index for soil physical quality and its use in Brazil. *Rev. Bras. Cienc. Do Solo* 38, 1–10. doi:10.1590/S0100-06832014000100001
- de Jong van Lier, Q., Gubiani, P.I., 2015. Beyond the “Least Limiting Water Range”: rethinking soil physics research in Brazil. *Rev. Bras. Cienc. do Solo* 39, 925–939. doi:10.1590/01000683rbc20140596
- de Jonge, H., Mittelmeijer-Hazeleger, M.C., 1996. Adsorption of CO₂ and N₂ on soil organic matter: Nature of porosity, surface area, and diffusion mechanisms. *Environ. Sci. Technol.* 30, 408–413. doi:10.1021/es950043t
- Delage, P., Pellerin, F.M., 1984. Influence de la lyophilisation sur la structure d’une argile sensible du Québec. *Clay Miner.* 19, 151–160. doi:10.1180/claymin.1984.019.2.03
- Della Vecchia, G., Dieudonné, A.C., Jommi, C., Charlier, R., 2015. Accounting for evolving pore size distribution in water retention models for compacted clays. *Int. J. Numer. Anal. Methods Geomech.* 39, 702–723. doi:10.1002/nag.2326
- Denef, K., Six, J., Merckx, R., Paustian, K., 2004. Carbon sequestration in microaggregates of no-tillage soils with different clay mineralogy. *Soil Sci. Soc. Am. J.* 68, 1935–1944. doi:10.2136/sssaj2004.1935
- Denef, K., Zotarelli, L., Boddey, R.M., Six, J., 2007. Microaggregate-associated carbon as a diagnostic fraction for management-induced changes in soil organic carbon in two Oxisols. *Soil Biol. Biochem.* 39, 1165–1172. doi:10.1016/j.soilbio.2006.12.024
- Destain, M.F., Roisin, C., Dalcq, A.S., Mercatoris, B.C.N., 2016. Effect of wheel traffic on the physical properties of a Luvisol. *Geoderma* 262, 276–284. doi:10.1016/j.geoderma.2015.08.028
- Dexter, A.R., 2004a. Soil physical quality Part I. Theory, effects of soil texture, density, and organic matter, and effects on root growth. *Geoderma* 120, 201–214. doi:10.1016/j.geoderma.2003.09.004
- Dexter, A.R., 2004b. Soil physical quality: Part II. Friability, tillage, tith and hard-setting. *Geoderma* 120, 215–225. doi:10.1016/j.geoderma.2003.09.005

- Dexter, A.R., 2004c. Soil physical quality. Part III: Unsaturated hydraulic conductivity and general conclusions about S-theory. *Geoderma* 120, 227–239. doi:10.1016/j.geoderma.2003.09.006
- Dexter, A.R., 1988. Advances in characterization of soil structure. *Soil Tillage Res.* 11, 199–238. doi:10.1016/0167-1987(88)90002-5
- Díaz-Zorita, M., Perfect, E., Grove, J.H., 2002. Disruptive methods for assessing soil structure. *Soil Tillage Res.* 64, 3–22. doi:10.1016/S0167-1987(01)00254-9
- Drury, C.F., Yang, X.M., Reynolds, W.D., Tan, C.S., 2004. Influence of crop rotation and aggregate size on carbon dioxide production and denitrification. *Soil Tillage Res.* 79, 87–100. doi:10.1016/j.still.2004.03.020
- Echeverría, J.C., Morera, M.T., Mazkarian, C., Garrido, J.J., 1999. Characterization of the porous structure of soils: adsorption of nitrogen (77K) and carbon dioxide (273K), and mercury porosimetry. *Eur. J. Soil Sci.* 50, 497–503. doi:10.1046/j.1365-2389.1999.00261.x
- Eck, D. V., Qin, M., Hirmas, D.R., Giménez, D., Brunzell, N.A., 2016. Relating quantitative soil structure metrics to saturated hydraulic conductivity. *Vadose Zone J.* 15. doi:10.2136/vzj2015.05.0083
- Elliott, E.T., Coleman, D.C., 1988. Let the soil work for us. *Ecol. Bull.* 39, 23–32.
- Eusterhues, K., Rumpel, C., Kögel-Knabner, I., 2005. Organo-mineral associations in sandy acid forest soils: importance of specific surface area, iron oxides and micropores. *Eur. J. Soil Sci.* 56, 753–763. doi:10.1111/j.1365-2389.2005.00710.x
- FAO, 2006. Guidelines for soil description, 4th ed. Food and Agriculture Organisation of the United Nations, Rome, Italy.
- Feeney, D.S., Crawford, J.W., Daniell, T., Hallett, P.D., Nunan, N., Ritz, K., Rivers, M., Young, I.M., 2006. Three-dimensional microorganization of the soil-root-microbe system. *Microb. Ecol.* 52, 151–158. doi:10.1007/s00248-006-9062-8
- Frisbie, J.A., Graham, R.C., Lee, B.D., 2014. A plaster cast method for determining soil bulk density. *Soil Sci.* 179, 103–106. doi:10.1097/SS.0000000000000044
- Garbout, A., Munkholm, L.J., Hansen, S.B., 2013. Tillage effects on topsoil structural quality assessed using X-ray CT, soil cores and visual soil evaluation. *Soil Tillage Res.* 128, 104–

109. doi:10.1016/j.still.2012.11.003

Giarola, N.F.B., da Silva, Á.P., Tormena, C.A., Guimarães, R.M.L., Ball, B.C., 2013. On the Visual Evaluation of Soil Structure: The Brazilian experience in Oxisols under no-tillage. *Soil Tillage Res.* 127, 60–64. doi:10.1016/j.still.2012.03.004

Giesche, H., 2006. Mercury porosimetry: A general (practical) overview. Part. Part. Syst. *Charact.* 23, 9–19. doi:10.1002/ppsc.200601009

Greiner, L., Keller, A., Grêt-Regamey, A., Papritz, A., 2017. Soil function assessment: review of methods for quantifying the contributions of soils to ecosystem services. *Land use policy* 69, 224–237. doi:10.1016/j.landusepol.2017.06.025

Guimarães, R.M.L., Ball, B.C., Tormena, C.A., 2011. Improvements in the visual evaluation of soil structure. *Soil Use Manag.* 27, 395–403. doi:10.1111/j.1475-2743.2011.00354.x

Guimarães, R.M.L., Ball, B.C., Tormena, C.A., Giarola, N.F.B., da Silva, Á.P., 2013. Relating visual evaluation of soil structure to other physical properties in soils of contrasting texture and management. *Soil Tillage Res.* 127, 92–99. doi:10.1016/j.still.2012.01.020

Guimarães, R.M.L., Lamandé, M., Munkholm, L.J., Ball, B.C., Keller, T., 2017. Opportunities and future directions for visual soil evaluation methods in soil structure research. *Soil Tillage Res.* 173, 104–113. doi:10.1016/j.still.2017.01.016

Hajnos, M., Lipiec, J., Świeboda, R., Sokołowska, Z., Witkowska-Walczak, B., 2006. Complete characterization of pore size distribution of tilled and orchard soil using water retention curve, mercury porosimetry, nitrogen adsorption, and water desorption methods. *Geoderma* 135, 307–314. doi:10.1016/j.geoderma.2006.01.010

Håkansson, I., 1990. A method for characterizing the state of compactness of the plough layer. *Soil Tillage Res.* 16, 105–120. doi:10.1016/0167-1987(90)90024-8

Håkansson, I., Lipiec, J., 2000. A review of the usefulness of relative bulk density values in studies of soil structure and compaction. *Soil Tillage Res.* 53, 71–85. doi:10.1016/S0167-1987(99)00095-1

Hall, M.R., Mooney, S.J., Sturrock, C., Matelloni, P., Rigby, S.P., 2013. An approach to characterisation of multi-scale pore geometry and correlation with moisture storage and transport coefficients in cement-stabilised soils. *Acta Geotech.* 8, 67–79. doi:10.1007/s11440-012-0178-3

- Han, L., Sun, K., Jin, J., Xing, B., 2015. Some concepts of soil organic carbon characteristics and mineral interaction from a review of literature. *Soil Biol. Biochem.* 94, 107–121. doi:10.1016/j.soilbio.2015.11.023
- Harrison, R.B., Adams, A.B., Licata, C., Flaming, B., Wagoner, G.L., Carpenter, P., Vance, E.D., 2003. Quantifying deep-soil and coarse-soil fractions: avoiding sampling bias. *Soil Sci. Soc. Am. J.* 67, 1602–1606.
- Hassink, J., Bouwman, L.A., Zwart, K.B., Brussaard, L., 1993. Relationships between habitable soil biota and mineralization rates in grassland soils. *Soil Biol. Biochem.* 25, 47–55. doi:10.1016/0038-0717(93)90240-C
- Haynes, R.J., 1993. Effect of sample pretreatment on aggregate stability measured by wet sieving or turbidimetry on soils of different cropping history. *J. Soil Sci.* 44, 261–270. doi:10.1111/j.1365-2389.1993.tb00450.x
- Heister, K., 2014. The measurement of the specific surface area of soils by gas and polar liquid adsorption methods - Limitations and potentials. *Geoderma* 216, 75–87. doi:10.1016/j.geoderma.2013.10.015
- Helliwell, J.R., Sturrock, C.J., Grayling, K.M., Tracy, S.R., Flavel, R.J., Young, I.M., Whalley, W.R., Mooney, S.J., 2013. Applications of X-ray computed tomography for examining biophysical interactions and structural development in soil systems: a review. *Eur. J. Soil Sci.* 64, 279–297. doi:10.1111/ejss.12028
- Herring, A.L., Andersson, L., Schlüter, S., Sheppard, A., Wildenschild, D., 2015. Efficiently engineering pore-scale processes: The role of force dominance and topology during nonwetting phase trapping in porous media. *Adv. Water Resour.* 79, 91–102. doi:10.1016/j.advwatres.2015.02.005
- Holmes, K.W., Wherrett, A., Keating, A., Murphy, D.V., 2011. Meeting bulk density sampling requirements efficiently to estimate soil carbon stocks. *Soil Res.* 49, 680–695. doi:10.1071/SR11161
- Horgan, G.W., 1998. Mathematical morphology for analysing soil structure from images. *Eur. J. Soil Sci.* 49, 161–173. doi:10.1046/j.1365-2389.1998.00160.x
- Igwe, C.A., Udegbonam, O.N., 2008. Soil properties influencing water-dispersible clay and silt in an Ultisol in southern Nigeria. *Int. Agrophysics* 22, 319–325.
- ISO 10930, 2012. Soil quality — Measurement of the stability of soil aggregates subjected to

the action of water.

- Jarvis, N., Larsbo, M., Koestel, J., 2017. Connectivity and percolation of structural pore networks in a cultivated silt loam soil quantified by X-ray tomography. *Geoderma* 287, 71–79. doi:10.1016/j.geoderma.2016.06.026
- Jozefaciuk, G., Czachor, H., Lamorski, K., Hajnos, M., Swieboda, R., Franus, W., 2015. Effect of humic acids, sesquioxides and silica on the pore system of silt aggregates measured by water vapour desorption, mercury intrusion and microtomography. *Eur. J. Soil Sci.* 66, 992–1001. doi:10.1111/ejss.12299
- Kaiser, K., Guggenberger, G., 2003. Mineral surfaces and soil organic matter. *Eur. J. Soil Sci.* 54, 219–236. doi:10.1046/j.1365-2389.2003.00544.x
- Katuwal, S., Norgaard, T., Moldrup, P., Lamandé, M., Wildenschild, D., de Jonge, L.W., 2015. Linking air and water transport in intact soils to macropore characteristics inferred from X-ray computed tomography. *Geoderma* 237–238, 9–20. doi:10.1016/j.geoderma.2014.08.006
- Kaufmann, M., Tobias, S., Schulin, R., 2010. Comparison of critical limits for crop plant growth based on different indicators for the state of soil compaction. *J. Plant Nutr. Soil Sci.* 173, 573–583. doi:10.1002/jpln.200900129
- Keller, T., Håkansson, I., 2010. Estimation of reference bulk density from soil particle size distribution and soil organic matter content. *Geoderma* 154, 398–406. doi:10.1016/j.geoderma.2009.11.013
- Kjaergaard, C., De Jonge, L.W., Moldrup, P., Schjønning, P., 2004. Water-dispersible colloids: effects of measurement method, clay content, initial soil matric potential, and wetting rate. *Vadose Zone J.* 3, 403–412. doi:10.2136/vzj2004.0403
- Kloubek, J., 1981. Hysteresis in porosimetry. *Powder Technol.* 29, 63–73. doi:10.1016/0032-5910(81)85005-X
- Kong, A.Y.Y., Six, J., Bryant, D.C., Denison, R.F., van Kessel, C., 2005. The relationship between carbon input, aggregation, and soil organic carbon stabilization in sustainable cropping systems. *Sci. Soc. Am. J.* 69, 1078–1085. doi:10.2136/sssaj2004.0215
- Kosugi, K., Dane, J.H., Hopmans, J.W., 2002. Parametric models, in: Dane, J.H., Topp, G.C. (Eds.), *Methods of Soil Analysis. Part 4. Physical Methods*. Soil Science Society of America, Book Series No. 5, Madison, WI., pp. 739–757.

- Kozak, E., Stawinski, J., Wierzchos, J., 1991. Reliability of mercury intrusion porosimetry results for soils. *Soil Sci.* 152, 405–413. doi:10.1097/00010694-199112000-00002
- Kravchenko, A.N., Guber, A.K., 2017. Soil pores and their contributions to soil carbon processes. *Geoderma* 287, 31–39. doi:10.1016/j.geoderma.2016.06.027
- Kravchenko, A.N., Negassa, W.C., Guber, A.K., Rivers, M.L., 2015. Protection of soil carbon within macro-aggregates depends on intra-aggregate pore characteristics. *Sci. Rep.* 5, 16261. doi:10.1038/srep16261
- Krull, E.S., Baldock, J.A., Skjemstad, J.O., 2003. Importance of mechanisms and processes of the stabilisation of soil organic matter for modelling carbon turnover. *Funct. Plant Biol.* 30, 207–222. doi:10.1071/FP02085
- Kuncoro, P.H., Koga, K., Satta, N., Muto, Y., 2014. A study on the effect of compaction on transport properties of soil gas and water. II: Soil pore structure indices. *Soil Tillage Res.* 143, 180–187. doi:10.1016/j.still.2014.01.008
- Larsbo, M., Koestel, J., Jarvis, N., 2014. Relations between macropore network characteristics and the degree of preferential solute transport. *Hydrol. Earth Syst. Sci.* 18, 5255–5269. doi:10.5194/hess-18-5255-2014
- Larsbo, M., Koestel, J., Kätterer, T., Jarvis, N., 2016. Preferential transport in macropores is reduced by soil organic carbon. *Vadose Zone J.* 15. doi:10.2136/vzj2016.03.0021
- Laundré, J.W., 1989. Estimating soil bulk-density with expanding polyurethane foam. *Soil Sci.* 147, 223–224. doi:10.1097/00010694-198903000-00009
- Lawrence, G.P., 1978. Stability of soil pores during mercury intrusion porosimetry. *J. Soil Sci.* 29, 299–304.
- Le Bissonnais, Y., 1996. Aggregate stability and assessment of soil crustability and erodibility : I. Theory and methodology. *Eur. J. Soil Sci.* 47, 425–437. doi:10.1111/j.1365-2389.1996.tb01843.x
- Lehmann, P., Wyss, P., Flisch, A., Lehmann, E., Vontobel, P., Krafczyk, M., Kaestner, A., Beckmann, F., Gygi, A., Flüher, H., 2006. Tomographical imaging and mathematical description of porous media used for the prediction of fluid distribution. *Vadose Zone J.* 5, 80–97. doi:10.2136/vzj2004.0177
- Letey, J., 1991. The study of soil structure - Science or art. *Soil Res.* 29, 699–707.

doi:10.1071/SR9910699

- Lowell, S., Shields, J.E., Thomas, M.A., Thommes, M., 2004. Characterization of porous solids and powders: surface area, pore size and density. Kluwer Academic Publishers, Dordrecht, The Netherlands. doi:10.1007/978-1-4020-2303-3
- Lu, Y., Liu, X., Heitman, J., Horton, R., Ren, T., 2016. Determining soil bulk density with thermo-time domain reflectometry: a thermal conductivity-based approach. *Soil Sci. Soc. Am. J.* 80, 48–54. doi:10.2136/sssaj2015.08.0315
- Luo, L., Lin, H., Schmidt, J., 2010. Quantitative relationships between soil macropore characteristics and preferential flow and transport. *Soil Sci. Soc. Am. J.* 74, 1929–1937. doi:10.2136/sssaj2010.0062
- Mangalassery, S., Sjögersten, S., Sparkes, D.L., Sturrock, C.J., Mooney, S.J., 2013. The effect of soil aggregate size on pore structure and its consequence on emission of greenhouse gases. *Soil Tillage Res.* 132, 39–46. doi:10.1016/j.still.2013.05.003
- Mayer, L.M., Schick, L.L., Hardy, K.R., Wagai, R., McCarthy, J., 2004. Organic matter in small mesopores in sediments and soils. *Geochim. Cosmochim. Acta* 68, 3863–3872. doi:10.1016/j.gca.2004.03.019
- McKenzie, D.C., 2001. Rapid assessment of soil compaction damage. I. The SOILpak score, a semi-quantitative measure of soil structural form. *Aust. J. Soil Res.* 39, 117–125. doi:10.1071/SR99116
- Moebius, B.N., van Es, H.M., Schindelbeck, R.R., Idowu, O.J., Clune, D.J., Thies, J.E., 2007. Evaluation of laboratory-measured soil properties as indicators of soil physical quality. *Soil Sci.* 172, 895–912. doi:10.1097/ss.0b013e318154b520
- Moni, C., Rumpel, C., Virto, I., Chabbi, A., Chenu, C., 2010. Relative importance of sorption versus aggregation for organic matter storage in subsoil horizons of two contrasting soils. *J. Soil Sci.* 61, 958–969. doi:10.1111/j.1365-2389.2010.01307.x
- Mualem, Y., 1976. A new model for predicting the hydraulic conductivity of unsaturated porous media. *Water Resour. Res.* 12, 513–522. doi:10.1029/WR012i003p00513
- Mueller, L., Kay, B.D., Hu, C., Li, Y., Schindler, U., Behrendt, A., Shepherd, T.G., Ball, B.C., 2009. Visual assessment of soil structure: evaluation of methodologies on sites in Canada, China and Germany. Part I: Comparing visual methods and linking them with soil physical data and grain yield of cereals. *Soil Tillage Res.* 103, 178–187.

doi:10.1016/j.still.2008.12.015

- Munkholm, L.J., Heck, R.J., Deen, B., Zidar, T., 2016. Relationship between soil aggregate strength, shape and porosity for soils under different long-term management. *Geoderma* 268, 52–59. doi:10.1016/j.geoderma.2016.01.005
- Naderi-Boldaji, M., Keller, T., 2016. Degree of soil compactness is highly correlated with the soil physical quality index S. *Soil Tillage Res.* 159, 41–46. doi:10.1016/j.still.2016.01.010
- Naveed, M., Arthur, E., De Jonge, L.W., Tuller, M., Moldrup, P., 2014a. Pore structure of natural and regenerated soil aggregates: an X-ray computed tomography analysis. *Soil Sci. Soc. Am. J.* 78, 377–386. doi:10.2136/sssaj2013.06.0216
- Naveed, M., Moldrup, P., Vogel, H.J., Lamandé, M., Wildenschild, D., Tuller, M., de Jonge, L.W., 2014b. Impact of long-term fertilization practice on soil structure evolution. *Geoderma* 217–218, 181–189. doi:10.1016/j.geoderma.2013.12.001
- Nciizah, A.D., Wakindiki, I.I.C., 2015. Physical indicators of soil erosion, aggregate stability and erodibility. *Arch. Agron. Soil Sci.* 61, 827–842. doi:10.1080/03650340.2014.956660
- Negassa, W.C., Guber, A.K., Kravchenko, A.N., Marsh, T.L., Hildebrandt, B., Rivers, M.L., 2015. Properties of soil pore space regulate pathways of plant residue decomposition and community structure of associated bacteria. *PLoS One* 10, 1–22. doi:10.1371/journal.pone.0123999
- Newell-Price, J.P., Whittingham, M.J., Chambers, B.J., Peel, S., 2013. Visual soil evaluation in relation to measured soil physical properties in a survey of grassland soil compaction in England and Wales. *Soil Tillage Res.* 127, 65–73. doi:10.1016/j.still.2012.03.003
- Neyshabouri, M.R., Kazemi, Z., Oustan, S., Moghaddam, M., 2014. PTFs for predicting LLWR from various soil attributes including cementing agents. *Geoderma* 226–227, 179–187. doi:10.1016/j.geoderma.2014.02.008
- Nimmo, J.R., 2005. Porosity and pore size distribution, in: *Encyclopedia of Soils in the Environment*. Elsevier, London, pp. 295–303. doi:10.1016/B0-12-348530-4/00404-5
- Oades, J.M., 1984. Soil organic matter and structural stability: mechanisms and implications for management. *Plant Soil* 76, 319–337. doi:10.1007/BF02205590
- Oades, J.M., Waters, A.G., 1991. Aggregate hierarchy in soils. *Soil Res.* 29, 815–828. doi:10.1071/SR9910815

- Otalvaro, I.F., Neto, M.P.C., Delage, P., Caicedo, B., 2016. Relationship between soil structure and water retention properties in a residual compacted soil. *Eng. Geol.* 205, 73–80. doi:10.1016/j.enggeo.2016.02.016
- Pachepsky, Y., Rawls, W., 2003. Soil structure and pedotransfer functions. *Eur. J. Soil Sci.* 54, 443–451. doi:10.1046/j.1365-2389.2003.00485.x
- Page-Dumroese, D.S., Brown, R.E., Jurgensen, M.F., Mroz, G.D., 1999. Comparison of methods for determining bulk densities of rocky forest soils. *Soil Sci. Soc. Am. J.* 63, 379–383. doi:10.2136/sssaj1999.03615995006300020016x
- Pagliai, M., Vignozzi, N., 2002. The soil pore system as an indicator of soil quality. *Adv. GeoEcology* 35, 69–80.
- Pagliai, M., Vignozzi, N., Pellegrini, S., 2004. Soil structure and the effect of management practices. *Soil Tillage Res.* 79, 131–143. doi:10.1016/j.still.2004.07.002
- Paradelo, M., Katuwal, S., Moldrup, P., Norgaard, T., Herath, L., de Jonge, L.W., 2016. X-ray CT-derived soil characteristics explain varying air, water, and solute transport properties across a loamy field. *Vadose Zone J.* 15. doi:10.2136/vzj2015.07.0104
- Paradelo, R., van Oort, F., Chenu, C., 2013. Water-dispersible clay in bare fallow soils after 80 years of continuous fertilizer addition. *Geoderma* 200–201, 40–44. doi:10.1016/j.geoderma.2013.01.014
- Paz Ferreira, J., Miranda, J.G.V., Vidal Vázquez, E., 2010. Multifractal analysis of soil porosity based on mercury injection and nitrogen adsorption. *Vadose Zone J.* 9, 325–335. doi:10.2136/vzj2009.0090
- Peerlkamp, P.K., 1959. A visual method of soil structure evaluation. *Meded. van Landbouwhoges. en der Opzoekingsstn. van den Staat te Gent* 24, 216–221.
- Peng, X., Horn, R.F., Hallett, P.D., 2015. Soil structure and its functions in ecosystems: phase matter & scale matter. *Soil Tillage Res.* 146, 1–3. doi:10.1016/j.still.2014.10.017
- Peters, A., Durner, W., 2006. Improved estimation of soil water retention characteristics from hydrostatic column experiments. *Water Resour. Res.* 42. doi:10.1029/2006WR004952
- Pires, L.F., Bacchi, O.O.S., Reichardt, K., Timm, L.C., 2005. Application of gamma-ray computed tomography to analysis of soil structure before density evaluations. *Appl. Radiat. Isot.* 63, 505–11. doi:10.1016/j.apradiso.2005.03.019

- Pohlmeier, A., Oros-Peusquens, A., Javaux, M., Menzel, M.I., Vanderborght, J., Kaffanke, J., Romanzetti, S., Lindenmair, J., Vereecken, H., Shah, N.J., 2008. Changes in soil water content resulting from *Ricinus* root uptake monitored by magnetic resonance imaging. *Vadose Zone J.* 7, 1010–1017. doi:10.2136/vzj2007.0110
- Pulido Moncada, M., Ball, B.C., Gabriels, D., Lobo, D., Cornelis, W.M., 2014a. Evaluation of soil physical quality index S for some tropical and temperate medium-textured soils. *Soil Sci. Soc. Am. J.* 79, 9–19. doi:10.2136/sssaj2014.06.0259
- Pulido Moncada, M., Gabriels, D., Cornelis, W., Lobo, D., 2013. Comparing aggregate stability tests for soil physical quality indicators. *L. Degrad. Dev.* 26, 843–852. doi:10.1002/ldr.2225
- Pulido Moncada, M., Gabriels, D., Lobo, D., Rey, J.C., Cornelis, W.M., 2014b. Visual field assessment of soil structural quality in tropical soils. *Soil Tillage Res.* 139, 8–18. doi:10.1016/j.still.2014.01.002
- Pulido Moncada, M., Helwig Penning, L., Timm, L.C., Gabriels, D., Cornelis, W.M., 2014c. Visual examinations and soil physical and hydraulic properties for assessing soil structural quality of soils with contrasting textures and land uses. *Soil Tillage Res.* 140, 20–28. doi:10.1016/j.still.2014.02.009
- Rabbi, S.M.F., Daniel, H., Lockwood, P. V., Macdonald, C., Pereg, L., Tighe, M., Wilson, B.R., Young, I.M., 2016. Physical soil architectural traits are functionally linked to carbon decomposition and bacterial diversity. *Sci. Rep.* 6, 33012. doi:10.1038/srep33012
- Rabot, E., Lacoste, M., Hénault, C., Cousin, I., 2015. Using X-ray computed tomography to describe the dynamics of nitrous oxide emissions during soil drying. *Vadose Zone J.* 14. doi:10.2136/vzj2014.12.0177
- Ragab, R., Feyen, J., Hillel, D., 1982. Effect of the method for determining pore size distribution on prediction of the hydraulic conductivity function and of infiltration. *Soil Sci.* 134, 141–145. doi:10.1097/00010694-198208000-00009
- Ravikovitch, P.I., Bogan, B.W., Neimark, A. V., 2005. Nitrogen and carbon dioxide adsorption by soils. *Environ. Sci. Technol.* 39, 4990–4995. doi:10.1021/es048307b
- Regelink, I.C., Stoof, C.R., Rouseva, S., Weng, L., Lair, G.J., Kram, P., Nikolaidis, N.P., Kercheva, M., Banwart, S., Comans, R.N.J., 2015. Linkages between aggregate formation, porosity and soil chemical properties. *Geoderma* 247–248, 24–37.

doi:10.1016/j.geoderma.2015.01.022

- Reichert, J.M., Suzuki, L.E.A.S., Reinert, D.J., Horn, R., Håkansson, I., 2009. Reference bulk density and critical degree-of-compactness for no-till crop production in subtropical highly weathered soils. *Soil Tillage Res.* 102, 242–254. doi:10.1016/j.still.2008.07.002
- Reinhart, K.O., Nichols, K.A., Petersen, M., Vermeire, L.T., 2015. Soil aggregate stability was an uncertain predictor of ecosystem functioning in a temperate and semiarid grassland. *Ecosphere* 6, 1–16. doi:10.1890/ES15-00056.1
- Renard, P., Allard, D., 2013. Connectivity metrics for subsurface flow and transport. *Adv. Water Resour.* 51, 168–196. doi:10.1016/j.advwatres.2011.12.001
- Renger, M., 1970. Über den Einfluss der Dränung auf das Gefüge und die Wasserdurchlässigkeit bindiger Böden. *Mitteilungen der Dtsch. Bodenkundlichen Gesellschaft* 11, 23–28.
- Renger, M., Bohne, K., Facklam, M., Harrach, T., Riek, W., Schäfer, W., Wessolek, G., Zacharias, S., 2008. Ergebnisse und Vorschläge der DBG-Arbeitsgruppe “Kennwerte des Bodengefüges” zur Schätzung bodenphysikalischer Kennwerte. Berlin.
- Reynolds, W.D., Drury, C.F., Tan, C.S., Fox, C.A., Yang, X.M., 2009. Use of indicators and pore volume-function characteristics to quantify soil physical quality. *Geoderma* 152, 252–263. doi:10.1016/j.geoderma.2009.06.009
- Richard, G., Cousin, I., Sillon, J.F., Bruand, A., Guérif, J., 2001. Effect of compaction on soil porosity: consequences on hydraulic properties. *Eur. J. Soil Sci.* 52, 49–58. doi:10.1046/j.1365-2389.2001.00357.x
- Roger-Estrade, J., Richard, G., Caneill, J., Boizard, H., Coquet, Y., Defosse, P., Manichon, H., 2004. Morphological characterisation of soil structure in tilled fields: from a diagnosis method to the modelling of structural changes over time. *Soil Tillage Res.* 79, 33–49. doi:10.1016/j.still.2004.03.009
- Romero, E., Simms, P.H., 2008. Microstructure investigation in unsaturated soils: a review with special attention to contribution of mercury intrusion porosimetry and environmental scanning electron microscopy. *Geotech. Geol. Eng.* 26, 705–727. doi:10.1007/s10706-008-9204-5
- Rossi, A.M., Hirmas, D.R., Graham, R.C., Sternberg, P.D., 2008. Bulk density determination by automated three-dimensional laser scanning. *Soil Sci. Soc. Am. J.* 72, 1591–1593.

doi:10.2136/sssaj2008.0072N

- Ruamps, L.S., Nunan, N., Chenu, C., 2011. Microbial biogeography at the soil pore scale. *Soil Biol. Biochem.* 43, 280–286. doi:10.1016/j.soilbio.2010.10.010
- Rücknagel, J., Hofmann, B., Paul, R., Christen, O., Hülsbergen, K.J., 2007. Estimating precompression stress of structured soils on the basis of aggregate density and dry bulk density. *Soil Tillage Res.* 92, 213–220. doi:10.1016/j.still.2006.03.004
- Sandin, M., Koestel, J., Jarvis, N., Larsbo, M., 2017. Post-tillage evolution of structural pore space and saturated and near-saturated hydraulic conductivity in a clay loam soil. *Soil Tillage Res.* 165, 161–168. doi:10.1016/j.still.2016.08.004
- Schaap, J.D., Lehmann, P., Kaestner, A., Vontobel, P., Hassanein, R., Frei, G., de Rooij, G.H., Lehmann, E., Flühler, H., 2008. Measuring the effect of structural connectivity on the water dynamics in heterogeneous porous media using speedy neutron tomography. *Adv. Water Resour.* 31, 1233–1241. doi:10.1016/j.advwatres.2008.04.014
- Schlüter, S., Sheppard, A., Brown, K., Wildenschild, D., 2014. Image processing of multiphase images obtained via X-ray microtomography: a review. *Water Resour. Res.* 50, 3615–3639. doi:10.1002/2014WR015256
- Schlüter, S., Vogel, H.J., 2016. Analysis of soil structure turnover with garnet particles and X-ray microtomography. *PLoS One* 11, e0159948. doi:10.1371/journal.pone.0159948
- Schlüter, S., Weller, U., Vogel, H.J., 2011. Soil-structure development including seasonal dynamics in a long-term fertilization experiment. *J. Plant Nutr. Soil Sci.* 174, 395–403. doi:10.1002/jpln.201000103
- Schoeneberger, P.J., Wysocki, D.A., Benham, E.C., Soil Survey Staff, 2012. Field book for describing and sampling soils, v. 3.0. Natural Resources Conservation Service, National Soil Survey Center, Lincoln, NE.
- Séquaris, J.M., Guisado, G., Magarinos, M., Moreno, C., Burauel, P., Narres, H.D., Vereecken, H., 2010. Organic-carbon fractions in an agricultural topsoil assessed by the determination of the soil mineral surface area. *J. Plant Nutr. Soil Sci.* 173, 699–705. doi:10.1002/jpln.200800224
- Seybold, C.A., Mausbach, M.J., Karlen, D.L., Rogers, H.H., 1998. Quantification of soil quality, in: Lal, R., Kimble, J.M., Follet, R.F., Stewart, B.A. (Eds.), *Soil Processes and the Carbon Cycle*. CRC Press LLC, Boca Raton, FL, pp. 387–404.

- Shepherd, T.G., 2009. Visual soil assessment. Volume 1. Field guide for pastoral grazing and cropping on flat to rolling country, 2nd ed. Horizons Regional Council, Palmerston North.
- Shepherd, T.G., 2003. Assessing soil quality using visual soil assessment, in: Currie, L.D., Hanly, J.A. (Eds.), Tools for Nutrient and Pollutant Management: Applications to Agriculture and Environmental Quality. Fertilizer and Lime Research Centre, Massey University, Palmerston North, pp. 153–166.
- Shepherd, T.G., 2000. Visual Soil Assessment. Volume 1. Field guide for cropping and pastoral grazing on flat to rolling country. horizons.mw & Landcare Research, Palmerston North.
- Shepherd, T.G., Stagnari, F., Pisante, M., Benites, J., 2008. Visual soil assessment - Field guide for annual crops. Rome, Italy.
- Simms, P.H., Yanful, E.K., 2001. Measurement and estimation of pore shrinkage and pore distribution in a clayey till during soil-water characteristic curve tests. *Can. Geotech. J.* 38, 741–754. doi:10.1139/t01-014
- Sing, K.S.W., Everett, D.H., Haul, R.A.W., Moscou, L., Pierotti, R.A., Rouquerol, J., Siemieniewska, T., 2008. Reporting physisorption data for gas/solid systems, in: Handbook of Heterogeneous Catalysis. Wiley-VCH Verlag GmbH & Co. KGaA, pp. 1217–1230. doi:10.1002/9783527610044.hetcat0065
- Six, J., Bossuyt, H., Degryze, S., Deneff, K., 2004. A history of research on the link between (micro)aggregates, soil biota, and soil organic matter dynamics. *Soil Tillage Res.* 79, 7–31. doi:10.1016/j.still.2004.03.008
- Six, J., Conant, R.T., Paul, E.A., Paustian, K., 2002. Stabilization mechanisms of soil organic matter: implications for C-saturation of soils. *Plant Soil* 241, 155–176. doi:10.1023/A:1016125726789
- Six, J., Paustian, K., 2014. Aggregate-associated soil organic matter as an ecosystem property and a measurement tool. *Soil Biol. Biochem.* 68, A4–A9. doi:10.1016/j.soilbio.2013.06.014
- Skvortsova, E.B., Sanzharova, S.I., 2007. Micromorphometric features of pore space in the plow horizons of loamy soils. *Eurasian Soil Sci.* 40, 445–455. doi:10.1134/S1064229307040114
- Skvortsova, E.B., Utkaeva, V.F., 2008. Soil pore space arrangement as a geometric indicator of soil structure. *Eurasian Soil Sci.* 41, 1198–1204. doi:10.1134/S1064229308110082

- Sněhota, M., Císlarová, M., Amin, M.H.G., Hall, L.D., 2010. Tracing the entrapped air in heterogeneous soil by means of magnetic resonance imaging. *Vadose Zone J.* 9, 373–384. doi:10.2136/vzj2009.0103
- Soil Survey Staff, 2014. Soil survey field and laboratory methods manual. Soil survey investigations, report No. 51, v.2. U.S. Department of Agriculture, Natural Resources Conservation Service.
- Strong, D.T., De Wever, H., Merckx, R., Recous, S., 2004. Spatial location of carbon decomposition in the soil pore system. *Eur. J. Soil Sci.* 55, 739–750. doi:10.1111/j.1365-2389.2004.00639.x
- Thompson, M.L., McBride, J.F., Horton, R., 1985. Effects of drying treatments on porosity of soil materials. *Soil Sci. Soc. Am. J.* 49, 1360–1364. doi:10.2136/sssaj1985.03615995004900060006x
- Throop, H.L., Archer, S.R., Monger, H.C., Waltman, S., 2012. When bulk density methods matter: implications for estimating soil organic carbon pools in rocky soils. *J. Arid Environ.* 77, 66–71. doi:10.1016/j.jaridenv.2011.08.020
- Timm, L.C., Pires, L.F., Reichardt, K., Roveratti, R., Oliveira, J.C.M., Bacchi, O.O.S., 2005. Soil bulk density evaluation by conventional and nuclear methods. *Aust. J. Soil Res.* 43, 97–103. doi:10.1071/SR04054
- Tisdall, J.M., Oades, J.M., 1982. Organic matter and water-stable aggregates in soils. *J. Soil Sci.* 33, 141–163. doi:10.1111/j.1365-2389.1982.tb01755.x
- Toosi, E.R., Kravchenko, A.N., Mao, J., Quigley, M.Y., Rivers, M.L., 2017. Effects of management and pore characteristics on organic matter composition of macroaggregates: evidence from characterization of organic matter and imaging. *Eur. J. Soil Sci.* 68, 200–211. doi:10.1111/ejss.12411
- Tuller, M., Kulkarni, R., Fink, W., 2013. Segmentation of X-ray CT data of porous materials: a review of global and locally adaptive algorithms, in: Anderson, S.H., Hopmans, J.W. (Eds.), *Soil–Water–Root Processes: Advances in Tomography and Imaging*, SSSA Special Publication 61. The Soil Science Society of America, Inc., Madison, WI, pp. 157–182. doi:10.2136/sssaspecpub61.c8
- Tumlinson, L.G., Liu, H., Silk, W.K., Hopmans, J.W., 2008. Thermal neutron computed tomography of soil water and plant roots. *Soil Sci. Soc. Am. J.* 72, 1234–1242.

doi:10.2136/sssaj2007.0302

Uteau, D., Pagenkemper, S.K., Peth, S., Horn, R., 2013. Aggregate and soil clod volume measurement: a method comparison. *Soil Sci. Soc. Am. J.* 77, 60–63. doi:10.2136/sssaj2012.0227n

Van Brakel, J., Modrý, S., Svatá, M., 1981. Mercury porosimetry: state of the art. *Powder Technol.* 29, 1–12. doi:10.1016/0032-5910(81)85001-2

van Genuchten, M.T., 1980. A closed-form equation for predicting the hydraulic conductivity of unsaturated soils. *Soil Sci. Soc. Am. J.* 44, 892–898. doi:10.2136/sssaj1980.03615995004400050002x

Vereecken, H., Weynants, M., Javaux, M., Pachepsky, Y., Schaap, M.G., Van Genuchten, M.T., 2010. Using pedotransfer functions to estimate the van Genuchten–Mualem soil hydraulic properties: a review. *Vadose Zone J.* 9, 795–820. doi:10.2136/vzj2010.0045

Vincent, K.R., Chadwick, O.A., 1994. Synthesizing bulk density for soils with abundant rock fragments. *Soil Sci. Soc. Am. J.* 58, 455–464. doi:10.2136/sssaj1994.03615995005800020030x

Virto, I., Barré, P., Chenu, C., 2008. Microaggregation and organic matter storage at the silt-size scale. *Geoderma* 146, 326–335. doi:10.1016/j.geoderma.2008.05.021

Vogel, H.J., 2000. A numerical experiment on pore size, pore connectivity, water retention, permeability, and solute transport using network models. *Eur. J. Soil Sci.* 51, 99–105. doi:10.1046/j.1365-2389.2000.00275.x

Vogel, H.J., Cousin, I., Roth, K., 2002. Quantification of pore structure and gas diffusion as a function of scale. *Eur. J. Soil Sci.* 53, 465–473. doi:10.1046/j.1365-2389.2002.00457.x

Vogel, H.J., Weller, U., Schlüter, S., 2010. Quantification of soil structure based on Minkowski functions. *Comput. Geosci.* 36, 1236–1245. doi:10.1016/j.cageo.2010.03.007

Wallace, K.J., 2007. Classification of ecosystem services: Problems and solutions. *Biol. Conserv.* 139, 235–246. doi:10.1016/j.biocon.2007.07.015

Wildenschild, D., Hopmans, J.W., Vaz, C.M.P., Rivers, M.L., Rikard, D., Christensen, B.S.B., 2002. Using X-ray computed tomography in hydrology: systems, resolutions, and limitations. *J. Hydrol.* 267, 285–297. doi:10.1016/S0022-1694(02)00157-9

Wildenschild, D., Sheppard, A.P., 2013. X-ray imaging and analysis techniques for quantifying

- pore-scale structure and processes in subsurface porous medium systems. *Adv. Water Resour.* 51, 217–246. doi:10.1016/j.advwatres.2012.07.018
- Young, I.M., Crawford, J.W., Nunan, N., Otten, W., Spiers, A., 2008. Microbial distribution in soils: physics and scaling, in: Sparks, D.L. (Ed.), *Advances in Agronomy*. Academic Press, Burlington, pp. 81–121. doi:10.1016/S0065-2113(08)00604-4
- Young, I.M., Crawford, J.W., Rappoldt, C., 2001. New methods and models for characterising structural heterogeneity of soil. *Soil Tillage Res.* 61, 33–45. doi:10.1016/S0167-1987(01)00188-X
- Zachara, J., Brantley, S., Chorover, J., Ewing, R., Kerisit, S., Liu, C., Perfect, E., Rother, G., Stack, A., 2016. Internal domains of natural porous media revealed: critical locations for transport, storage, and chemical reaction. *Environ. Sci. Technol.* 50, 2811–2829. doi:10.1021/acs.est.5b05015
- Zacharias, S., Bohne, K., 2008. Attempt of a flux-based evaluation of field capacity. *J. Plant Nutr. Soil Sci.* 171, 399–408. doi:10.1002/jpln.200625168
- Zong, Y., Yu, X., Zhu, M., Lu, S., 2015. Characterizing soil pore structure using nitrogen adsorption, mercury intrusion porosimetry, and synchrotron-radiation-based X-ray computed microtomography techniques. *J. Soils Sediments* 15, 302–312. doi:10.1007/s11368-014-0995-0

Figures



Figure 1: Visual key for scoring soil structure after a drop-shatter test. (a) Good, (b) moderate, and (c) poor physical condition. Reprinted from Shepherd et al. (2008).

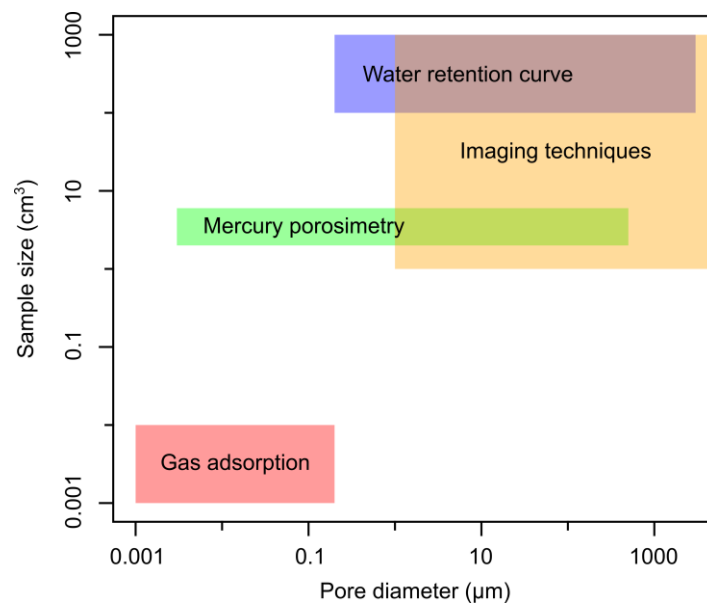


Figure 2: Comparison of the sample sizes and pore sizes investigated with the different methods to characterize soil pore space. Both axes are represented with a logarithmic scale.

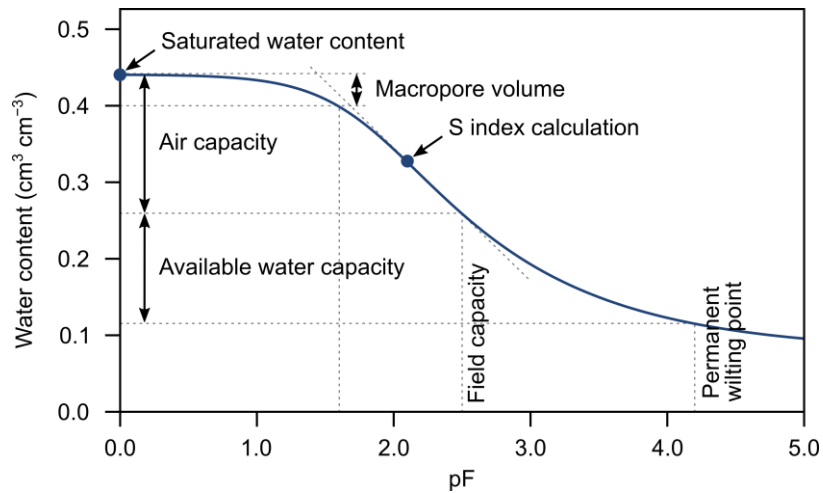


Figure 3: Indicators derived from the water retention curve.

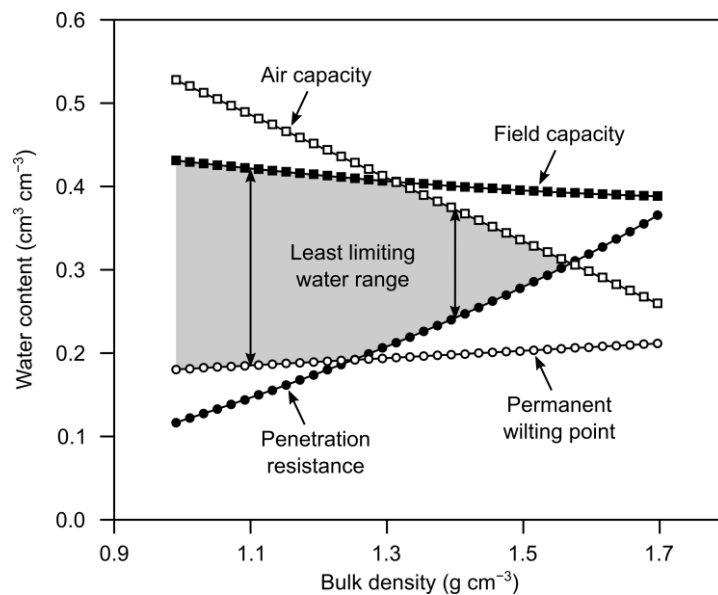


Figure 4: Least limiting water range (LLWR) of a loamy soil as function of bulk density. The left arrow represents the LLWR at the bulk density of 1.1 g cm^{-3} , where plant growth is limited by field capacity and permanent wilting point. The right arrow represents the LLWR at the bulk density of 1.4 g cm^{-3} , where high penetration resistance and low air capacity further reduce the LLWR. Redrawn from Kaufmann et al. (2010).

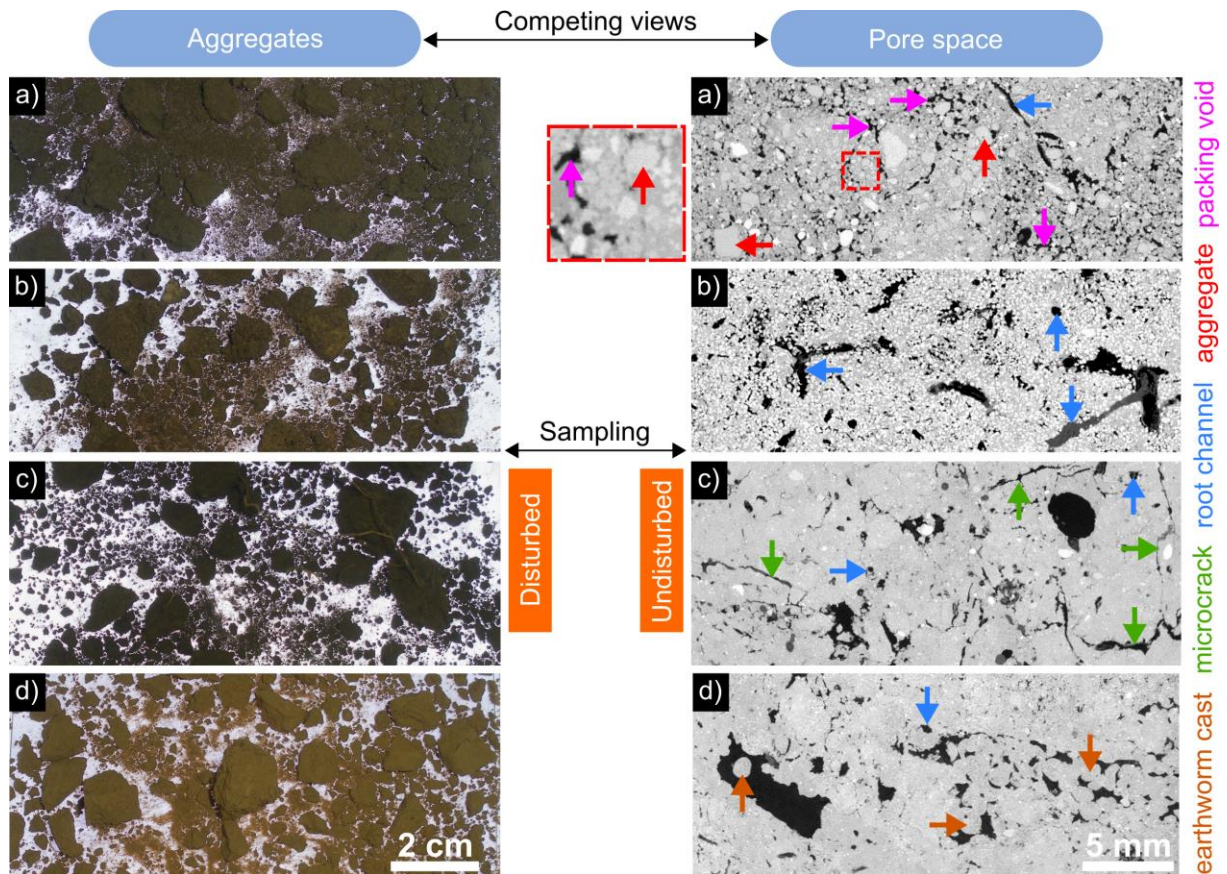


Figure 5: Summary of two competing views: the aggregate perspective and the pore space perspective. (a) Kühnfeld, Halle, Germany (continuous maize, conventional tillage, topsoil, 63% sand, 25% silt, 12% clay), (b) Hadera, Israel (orchard, topsoil, 65% sand, 16% silt, 19% clay), (c) Bad Lauchstädt, Germany (grassland, topsoil, 12% sand, 68% silt, 20% clay), (d) Garzweiler, Germany (crop rotation, below plow layer, 5% sand, 81% silt, 14% clay).

Tables

Table 1: Comparison of different measurement methods and indicators of soil structure.

Measurement method	Indicator	Sample size	Pore size observed	Level of expertise ^a	Reproducibility ^b	Duration ^c	Cost	Measure	Methodological limitations
Whole profile evaluation	Grade, size, shape of peds	Horizon	> 200 μm	High	Medium	Half an hour + pit	Low	Qualitative	<ul style="list-style-type: none"> - Subjective - Depends on soil texture and moisture
Topsoil evaluation	Visual evaluation score	Full size of a spade and \approx 20 cm-thick	> 200 μm	Medium	Medium	Half an hour	Low	Semi-quantitative	<ul style="list-style-type: none"> - Subjective - Depends on soil texture, moisture, and biological activity - Difficulty in breaking soil manually along planes of weakness - Compaction may occur during the drop-shatter test or by breaking soil manually
Bulk density	Bulk density	Hundreds cm^3 to hundreds dm^3	-	Low	High	Half an hour + drying	Low	Quantitative	<ul style="list-style-type: none"> - Difficulties with soils with abundant rock fragments, plant roots, or residues - Depends on soil moisture - Compaction may occur with the core method - Inadequate representation of large pores with the clod method
	Degree of compactness			Medium	Medium	A few hours + drying	Medium		<ul style="list-style-type: none"> - No standard method to evaluate the reference BD - Not satisfying for organic soils, doubt for sandy soils
	Packing density			Low	High	A few hours +drying	Low		<ul style="list-style-type: none"> - (Poorly explored so far)
Aggregate size distribution and stability	Stability index Aggregate size distribution Water-dispersible clay Microaggregates-within-macroaggregates	Tens to hundred g	-	Medium	Low	A few hours	Low	Quantitative	<ul style="list-style-type: none"> - Wide number of measurement methods - Unknown applied energy - Non-negligible effect of the type of sieving, duration, oscillation frequency, loading rate, number and size of sieves, storage duration, and pretreatment (moisture history)
Mercury porosimetry	Porosity Macroporosity Microporosity	A few cm^3	0.003 to 500 μm	Low	High	A few hours	Medium	Quantitative	<ul style="list-style-type: none"> - Assumes non-connected cylindrical pores - Ink-bottle effect - Contact angle of mercury with soil surface often unknown - Sample dried
Water retention curve	Porosity Macroporosity Microporosity Air capacity Relative field capacity Available water capacity LLWR S index	Hundreds cm^3 to dm^3	0.2 to 3000 μm	Medium	High	Days to weeks	Medium	Quantitative	<ul style="list-style-type: none"> - Assumes non-connected cylindrical pores - Ink-bottle effect - Adjustment of a model can introduce small errors

Gas adsorption	Specific surface area Mesoporosity (2–50 nm) Microporosity (< 2 nm)	1 to tens mm ³	0.001 to 0.2 μm	High	Medium	A few hours to days	Medium	Quantitative	- Assumes an idealized pore shape - Sample dried - N ₂ inadequate to characterize soils with high amounts of SOM
Imaging techniques (lab)	Porosity Macroporosity Microporosity Connectivity Pore orientation Pore shape	1 cm ³ to dm ³	A few μm to hundreds μm	High	Medium	A few hours	High	Quantitative	- Sensitive to the segmentation step and image resolution

^a High: several protocols exist to perform the measurement and/or to analyze the data, which need to be adapted for the case study, a dedicated training and experience is required; Medium: several protocols exist to perform the measurement and/or to analyze the data, which need to be adapted for the case study, but skills can be learned easily; Low: a protocol exist to perform the measurement and/or to analyze the data, skills can be learned easily.

^b Different operators characterize the same soil sample and choose between the different protocols available to perform the measurement and/or to analyze the data. The step of soil sampling is not taken into account. High: same results; Medium: same results to same trends; Low: same results to different trends.

^c We aimed at showing how labor-intensive the methods are for a single sample. The step of soil sampling is not taken into account.

Table 2: Comparison of indicators of soil structure to assess soil functions.

Measurement method	Indicator	Soil function					
		Biomass production	Storage and filtering of water	Storage and recycling of nutrients	Carbon storage	Habitat for biological activity	Physical stability and support
Whole profile evaluation	Ped grade		×				
	Ped size						
	Ped shape						
Topsoil evaluation	Visual evaluation score	×	×				×
Bulk density	Bulk density	(×)					×
	Degree of compactness	×	×				
	Packing density	×					
Aggregate size distribution and stability	Stability index		×	×			×
	Aggregate size distribution	×	×		×		×
	Water-dispersible clay		×	×			×
	Microaggregates-within-macroaggregates				×		
Mercury porosimetry	Porosity						
	Macroporosity					×	(×)
	Microporosity					×	
Water retention curve	Porosity		×				
	Macroporosity	×				×	
	Microporosity					×	
	Air capacity	×					
	Relative field capacity	×		×		×	
	Available water capacity	×	×				
	LLWR	(×)					
	S index	(×)	×				×
Gas adsorption	Specific surface area				(×)		
	Mesoporosity (2–50 nm)						
	Microporosity (< 2 nm)						
Imaging techniques	Porosity	×	×	(×)			×
	Macroporosity	×	×	(×)	×	×	
	Microporosity	×	×	(×)	×	×	
	Connectivity		×	(×)	×		×
	Pore orientation		×	(×)			
	Pore shape		×	(×)			

